Materials for Gasifier Heat Exchangers

Report No.
COAL R263
DTI/Pub
URN 04/1796

November 2004

by

P Kilgallon, N J Simms, and J E Oakey

Power Generation Technology Centre
Cranfield University,
Cranfield,
Bedfordshire
MK43 0AL

Tel: 01234 754258
Email: J.E.Oakey@cranfield.ac.uk

The work described in this report was carried out under contract as part of the DTI Cleaner Coal Research and Development Programme. The programme is managed by Mott MacDonald Ltd. The views and judgements expressed in this report are those of the contractor and do not necessarily reflect those of the DTI or Mott MacDonald Ltd

First published 2004

MATERIALS FOR GASIFIER HEAT EXCHANGERS

P Kilgallon, N J Simms, and J E Oakey, Power Generation Technology Centre,
Cranfield University, UK

SUMMARY

A wide variety of gasification systems are continuing to be developed around the world, including Integrated Gasification Combined Cycle (IGCC) and the UK developed Air Blown Gasification Cycle (ABGC) systems. Originally, these systems were developed to be fired on various grades of coal, but there is now interest in using a more diverse range of solid fuels (e.g. co-firing coal with waste or biomass, using low grade coals and heavy fuel oils) in order to reduce environmental impact and fuel costs.

All gasification technologies require a heat exchanger (often called either a syngas cooler or fuel gas cooler) between the gasifier and the gas cleaning system. The duty required from this heat exchanger varies depending on the type of gasifier, gas-cleaning requirements (e.g. hot dry cleaning or wet scrubbing) and steam cycle needs. However, gasifier hot gas path environments are potentially very aggressive for materials both during plant operation and off-line periods. This has the effect of imposing a temperature window for the safe operation of these heat exchangers (with current materials restricting their use to modest steam conditions and preventing their use as superheaters with commercially viable lives) and dictates that downtime corrosion control precautions are required during off-line periods. There are significant differences in the hot gas path environments between the various gasification systems and with different fuels, but unfortunately these just have the effect of changing the balance between different potential degradation modes arising from the gasification environments.

The project has assessed the potential corrosive effects of deposits formed on coal-fired and coal/waste co-fired gasifier fuel-gas/syngas heat exchangers in ABGC and IGCC systems. This has included determining the ranges of deposit compositions formed on heat exchangers with different fuels and quantitatively assessing the effects of such deposits on downtime corrosion (including the effects of potential preventative measures) and synergistic interactions. These activities have lead to the identification of combinations of fuels, operating conditions and materials that could produce rapid heat exchanger failures due to interactions with the deposits formed during the heat exchanger operation.

The following candidate gasifier heat exchanger alloys were investigated; AISI 316L, AISI 310, AISI 347H, Alloy 800, Sanicro 28, Haynes 160, Esshete 1250, Haynes 556, IN625 and T23. In terms of cost and performance Sanicro 28 appears to be the best choice for evaporative heat exchangers in the range of test conditions investigated.

CONTENTS

MATERIALS FOR GASIFIER HEAT EXCHANGERS

1. INTRODUCTION

A wide variety of gasification systems are continuing to be developed around the world, including Integrated Gasification Combined Cycle (IGCC) and the UK developed Air Blown Gasification Cycle (ABGC) systems. Originally, these systems were developed to be fired on various grades of coal, but there is now interest in using a more diverse range of solid fuels (e.g. co-firing coal with waste or biomass, using low grade coals and heavy fuel oils) in order to reduce environmental impact and fuel costs.

All gasification technologies require a heat exchanger (often called either a syngas cooler or fuel gas cooler) between the gasifier and the gas cleaning system. The duty required from this heat exchanger varies depending on the type of gasifier, gas-cleaning requirements (e.g. hot dry cleaning or wet scrubbing) and steam cycle needs. However, gasifier hot gas path environments are potentially very aggressive for materials both during plant operation and off-line periods. This has the effect of imposing a temperature window for the safe operation of these heat exchangers (with current materials restricting their use to modest steam conditions and preventing their use as superheaters with commercially viable lives) and dictates that downtime corrosion control precautions are required during off-line periods. There are significant differences in the hot gas path environments between the various gasification systems and with different fuels, but unfortunately these just have the effect of changing the balance between different potential degradation modes arising from the gasification environments.

2. AIMS AND OBJECTIVES

The overall aim of the project was to assess the potential corrosive effects of deposits formed on coal-fired and coal/waste co-fired gasifier fuel-gas/syngas heat exchangers in ABGC and IGCC systems, especially their effects on downtime corrosion (including the effects of preventative measures) and synergistic interactions.

Specific objectives of the project were:

- To determine the composition ranges of deposits formed on coal-fired and coal/waste co-fired ABGC and IGCC fuel-gas/syngas heat exchangers;
- To quantitatively assess the rates at which these deposits cause downtime corrosion and the effectiveness of proposed preventative measures;
- To assess the potential for the deposits that cause synergistic degradation (at high and low temperatures), and the resulting increase in materials damage rates;
- To identify safe exposure/operating conditions/materials that avoid rapid heat exchanger failures.

3. BACKGROUND

3.1. Technology

A number of coal gasification systems have been developed [1], based on different types of gasification processes, e.g. entrained flow, fixed bed, and fluidised bed. Variations on these processes may use either oxygen or air as their oxidant in the gasifier vessel and can be controlled to give varying degrees of conversion of the coal to fuel gas, from complete (>99% conversion) to partial (e.g. 75% conversion). Once generated, the fuel gases need to be cooled and cleaned before being burnt in gas turbines. It is possible to carry out the gas cleaning by water scrubbing the cooled fuel gases, but this leads to lower cycle efficiencies and requires the provision of a scrubbing and wastewater treatment facility, which generates liquid waste for later disposal. The first generation gasification systems have been built to use water scrubbing for gas cleaning. Hot dry gas cleaning, using barrier filters to remove particulates and catalysts/sorbents to remove gaseous species (e.g. sulphur, chlorine, ammonia), offer higher cycle efficiencies as well as lower capital and operating/disposal costs. However, hot dry gas cleaning is still at the developmental stage and so only parts of these processes are included in the latest demonstration plants, often as parts of sidestreams.

There are many significant differences between the various gasification systems [1], both in terms of the operation of the actual gasification process and the requirements for different downstream components with different ranges of operating conditions. These give rise to economic and efficiency differences between the systems that are beyond the scope of this report. However, from the perspective of materials performances and the optimum materials selection, the component operating conditions and the environments produced in each of the systems are critically important. Table 1 lists published bulk gas compositions produced by some of these gasification systems. Further differences arise from the minor and trace gas species that are both very important in determining materials performances, both through direct reaction and indirectly through deposit formations and subsequent reaction. The levels of the minor and trace gas species in these gasification systems are not readily available.

The majority of the coal gasification processes which have reached the pilot and demonstration plant scale are based on pressurised oxygen blown entrained flow slagging gasifiers, e.g. the Texaco, Dow, Shell (Figure 1), Prenflo and GSP processes [2]. In addition, air blown pressurised fluidised bed gasification (PFBG) processes have been developed by, for example, British Coal and HT-Winkler and offer improved fuel flexibility (e.g. a wider range of coals, co-firing with biomass).

Within Europe, demonstration scale gasification systems have been built based on the Shell gasification process (a 253MW plant at Buggenum, Holland, operated by Demkolec BV [2]) and on the Prenflo process (a 335MW plant at Puertollano, Spain, operated by Elcogas [3]). Both these systems use oxygen blown entrained slagging processes to gasify coal.

The use of partial gasification systems results in hybrid cycles, in which unburned carbon from the gasifier is burnt in a combustor to raise steam for the steam cycle. These cycles have many advantages in terms of efficiencies, staged construction, fuel flexibility (e.g. range of coals, co-firing with biomass) and availability of different parts of the system for power generation. British Coal's Air Blown Gasification Cycle (ABGC) [3] is an example of such a cycle. In this system, an air blown fluidised bed partial (~70% conversion) gasifier is used with a circulating fluidised bed as the char combustor (Figure 2). Similar hybrid 'partial' gasification/combustion cycles have been proposed by other companies, for example Foster Wheeler's

Carboniser/Pressurised Fluidised Bed Combustor (PFBC) Cycle [4] and ABB's second generation PFBC cycle [5].

All gasification technologies require a heat exchanger (often called either a syngas cooler or fuel gas cooler) between the gasifier and the gas cleaning system. The duty required from this heat exchanger varies depending on the type of gasifier, gas cleaning requirements (e.g. hot dry cleaning or wet scrubbing) and steam cycle needs. However, gasifier hot gas path environments are potentially very aggressive for materials both during plant operation and off-line periods. This has the effect of imposing a temperature window for the safe operation of these heat exchangers (with current materials restricting their use to modest steam conditions and preventing their use as superheaters with commercially viable lives). Thus, in different gasification systems evaporators are used to produce saturated steam at 10MPa/320°C with metal temperatures of 320-400°C depending on the syngas temperature [6]. It is expected that evaporator steam conditions will be raised to 18MPa/350°C, with corresponding metal temperatures of 380-450°C. Even at these steam conditions, highly alloyed materials such as alloy 800 (Fe-32Ni-20Cr) or Sanicro 28 (Fe-31Ni-27Cr-3Mo) need to be used to give economically viable heat exchanger lives [7]. However, some gasification cycles would be more efficient (and viable) if at least some superheating could be carried out by a heat exchanger in this location in the hot gas path: this would involve steam at temperatures of 500-550°C with corresponding metal temperatures of 550-600°C [6]. Both water tube and smoke tube heat exchanger designs are reported in the literature for gasifier heat exchangers: these radically different types of designs will have different characteristics in terms of deposit formations, due to the different gas flows around/through them.

3.2. Degradation Modes

The performance of materials in various simulated and real coal-gasification gases have been investigated by research groups in the US, Japan and Europe for more than 25 years. The initial generic studies investigated the performance of materials in a range of highly reducing atmospheres with varying levels of sulphidation at high temperatures. Later studies have tended to concentrate on higher alloyed materials and/or lower exposure temperature. Following plant experience, more recent studies have been targeted at increasingly realistic exposure simulations to match the degradation morphologies observed in practise.

There are several potential degradation processes for these environments [8-14], including:

- *elevated temperature gas phase induced corrosion* - this includes oxidation, sulphidation, carburisation/metal dusting and chlorination;
- *corrosion induced by surface deposits* - either particles from the gasifier, species condensed onto those particles or species condensed onto the component surfaces;
- *dewpoint corrosion* - induced by high temperature deposits becoming damp during plant idling, gaseous species (e.g. HCl, H_2S, etc) reacting with condensing water during idling (e.g. forming HCl and polythionic acids) or deposits forming on cooler gas path surfaces;
- *downtime corrosion* - induced by high temperature deposits becoming damp during plant shut-down, gaseous species (e.g. HCl, H_2S, etc) reacting with condensed water during plant shut-down (e.g. forming HCl and polythionic acids) or hygroscopic deposits being exposed to damp air during plant shut-downs (e.g. during the course of maintenance operations);
- *interaction of any of the above degradation modes with mechanical factors* - e.g. creep or fatigue, to produce synergistic degradation, e.g. creep-corrosion or corrosion-fatigue;
- *spallation of corrosion products* - important on the clean side of the filter unit from where spalled scale may enter the gas turbine and cause erosion damage.

In practise, several materials degradation modes will occur on each component in the hot gas path. In any one gasification system, different combinations of degradation modes will be found on components along the hot gas path due to differences in operating temperature and local plant environment (deposition, local gas composition, i.e. the extent of gas clean-up, gas temperature at that point in the system, component temperature, etc.).

The effects of the oxidation and sulphidation resistance of materials in coal gasification environments have been the subjects of several investigations over the past 30 years. However, much of the earlier work established that high operating temperatures would give unviable component lives, so that the more recent work gives more useful information regarding component lives at realistic operating temperatures (in particular work carried out by KEMA (Holland), Shell (USA) and British Coal (UK, in a DTI funded Clean Coal Project, C/00086). The other degradation mechanisms have received relatively little study to date, with KEMA and British Coal starting small studies on downtime corrosion and synergistic effects when plant operations started to highlight their importance with component failures. In any power generating system, whether a new technology or a development of an existing technology, it is vital that all components are reliable and give predictable service lives. The fuel gas/ syngas heat exchanger has to meet the current standard reliability and maintenance requirement of the rest of the plant. Unplanned outages for component failures are expensive and can give new/improved technologies bad reputations hindering or even preventing their introduction.

3.3. Gasifier Gas Compositions

The major components of gasifier fuel gas are CO, CO_2, H_2, H_2O, CH_4 and N_2, with typical minor components of H_2S, HCl, NH_3 and COS and a range of trace elements. The relative amounts of each component depend on the particular gasification process, temperature, pressure, fuel composition, air to fuel ratio and the extent of steam additions. Typical ranges for the major and minor components reported in the literature for coal gasification are given in Table 1. Gasifier gas compositions reported for waste or waste/coal firing generally only gave the major components and these are in the same range as reported for coal firing.

Fuel related considerations for a gasifier fuel gas fired gas turbine are calorific value, gas turbine fuel specifications and emissions regulations. Generally the oxygen blown systems have significantly higher levels of CO, H_2 and H_2S than air blown systems, the higher CO and H_2 levels give higher calorific value product gases (e.g. for biomass firing 10-15MJ/Nm^3 compared to 4-6MJ/Nm^3). Low calorific gas burners have been developed that work with the lower calorific value fuel gas produced by air blown gasifiers. In general, the fuels sulphur and chlorine levels are of greater concern for oxygen blown systems than air blown systems due to the higher H_2S, HCl and related species produced in the gasifier gas. The implications of trace elements in the fuel gas (and therefore in the fuel) are discussed in section 4.

Fuel specifications for gas turbines generally specify limits for solids, sulphur and trace elements such as lead, vanadium, calcium and alkali metals. Gasification of waste\coal mixtures could change the levels of these contaminants in the fuel gas compared to coal alone, for example, higher alkali metals but lower sulphur with wheat straw. Generally, no chloride limit is set in the fuel specifications or emission regulations. Typical HCl concentrations in coal fired air blown gasifiers range from <10 vpm up to 1000 vpm, wastes such as waste wood or straw can have much higher chloride levels. Meeting both the gas turbine fuel

specification and the emissions regulations can be achieved with existing technologies such as hot gas cleaning, in-bed capture etc.

3.4. Deposit Formation Mechanisms and Effects for Gasifier Heat Exchangers

In all gasification systems, the deposits that form on the heat exchangers are dependent on:

- the breakdown of the fuel;
- the subsequent passage of the particles, vapour and gas phase species through the hot gas path of gasification system;
- the physical design and operating conditions of the heat exchanger (e.g. gas and metal temperatures).

The detailed operation of the different types of gasifiers is beyond the scope of this report but has been well reviewed in a series of IEA Coal Reports [1, 15-16]. A schematic diagram of the breakdown of a piece of coal and subsequent types of reactions is given in Figure 3.

The passage of ash particles (either solid or molten) along the gasifier hot gas path depends on a combination of their size and stickiness as well as the design of the gasifier hot gas path. Some systems are designed to remove molten ash whilst others have cyclones to remove solid fly ash particles [1].

Once particles reach the heat exchanger, their deposition depends on the gas flow around the heat exchanger and its operating conditions (e.g. gas and surface temperatures). Deposition routes include:

- direct inertial impaction
- turbulent eddy diffusion
- brownian diffusion
- thermophoresis (when a temperature gradient is established in gas, small particles suspended in the gas migrate in the direction of decreasing temperature)

The first of these, direct inertial impaction, usually applies to particles larger than ~10μm, whilst the others apply to smaller particles [17].

The composition of the particles will be dependent on the fuel, but will usually include alumino-silicates and other minerals, the surfaces of some of these many have been enriched with elements condensing from the vapour phase (see below) and in many gasification systems there may be a significant unburned carbon content. For gasifiers using limestone or dolomite sorbents, there will be significant levels of calcium and magnesium compounds [18].

For vapour phase species, there are essentially two deposition routes onto heat exchanger surfaces:

- Condensation onto particles and subsequent particle deposition;
- Direct condensation onto the heat exchanger

In the later, direct condensation onto the heat exchanger, the temperatures of the heat exchanger and the local gas environment are critical, as is the composition of the local gas environment. It should be noted that whilst the bulk gas compositions will remain ‘frozen’ at the gasifier outlet composition (due to its rapid passage through the plant), the gas composition(s) within the boundary layers surrounding the heat exchangers can be closer to equilibrium due to their lower velocities and proximity to potentially catalytic surfaces.

The fate of the elements in gasification systems is summarised in Figure 4.

There are a number of potential deleterious effects due to deposit formation on gasifier heat exchangers as follows:

- blocking of gas paths around the heat exchanger
- reduction in heat transfer
- transport of corrosive species to the heat exchanger
- destabilisation of protective corrosion products
- formation of low melting point/fluxing compounds
- restriction of gas access to the heat exchanger surfaces
- moisture absorption leading to downtime or dewpoint corrosion

4. DEPOSIT FORMATION ON GASIFIER HOT GAS PATH COMPONENTS

4.1. Introduction

A literature search was carried out to gather together reported information on the formation of deposits in gasifier fuel gas/syngas heat exchangers. In light of the limited information on deposit compositions found in the literature and available from COST522 partners, this data gathering was extended to cover the volatilisation and condensation of trace element species in gasifier fuel gas paths, as this is the major route by which chemically aggressive deposits could be formed on heat exchanger surfaces. This yielded more useful information on potential heat exchanger deposit compositions. However, there were still obvious limitations in the information gathered, so a thermodynamic study (see section 5) was carried out to provide consistent data on the effects of pressure and gas compositions in an Air Blown Gasification Cycle (ABGC) and a Prenflo IGCC system.

4.2. Literature Data on Gasifier Heat Exchanger Deposit Compositions

Limited data has been reported on the compositions of deposits found on gasifier heat exchangers.

For the ABGC system, a DTI Coal Report [19] gave a detailed analysis (Table 2) for a deposit formed on cooled probes upstream of a hot gas filter unit (i.e. in the location of a gasifier heat exchanger in an ABGC system).

Later work on this spouted fluidised bed gasification plant showed that the deposits that formed could also contain significant levels of As, Cd and Se.

Literature reports of the performance of materials in heat exchangers and probes in other gasification systems also report the presence of significant levels of Pb, As, Se, Ge, and Sb [20]. Again significant levels (up to 80 weight % in EDX analysis of elements with atomic weights heavier than Na) of these elements were observed (Figure 5), even though these elements would only have been present in the fuel gas stream at trace levels (<100 ppm).

Tests to investigate downtime corrosion of materials in coal gasification environments have reported different simulations of gasifier heat exchanger deposits (Table 3). These compositions have been produced by EPRI [21] and KEMA [22], from their experience of

entrained gasification processes, and British Coal, from their experience of a fluidised bed partial gasifier [23]. Other research laboratories have used these deposit compositions in various downtime corrosion test programmes [24]

Figures 6 and 7 have been produced to summarise the currently available literature on gasifier heat exchanger deposit formation.

As so many potentially damaging elements are volatile in coal gasification environments, and only limited data has been found on heat exchanger deposit compositions, the fate of these elements are considered in detail in section 5 of this report.

5. REVIEW OF GASIFIER TRACE ELEMENT PARTITIONING

5.1. Introduction

The fuels used in a gasifier system will provide a source of trace elements that are available for transport through the hot gas path. It is clear from available plant data that a range of vapour phase species do pass through the hot gas paths of gasification systems. Early studies of the volatility of trace elements within gasification and combustion systems have tried to classify their behaviour very broadly as shown in Figure 8. As more studies [25-35] have been carried out it has become evident that while the behaviour of trace elements in combustion systems lends itself well to a broad classification, trace element behaviour in gasification systems is not so clear.

Trace elements are introduced into the gasification system in the fuel and in sorbents and from degradation of system components. Trace elements within the gasifier may be retained in the slag/ash or leave in the fuel gas either associated with particulates or in the vapour phase. The fate of trace elements in a gasifier system is shown schematically in Figure 4. In this report the partitioning of trace elements in gasification systems is reviewed in terms of actual partitioning data and results from thermodynamic studies.

5.2. Review of Thermodynamic Studies On Trace Elements in Gasifier Environments

5.2.1. Introduction

There are many thermodynamic computer packages available that can be used to carry out thermodynamic trace element analysis. The results obtained may be dependent on the computer package used and definitely will be dependent on the species included and the available thermodynamic data. Frandsen [37] compared a number of packages using a combustor model and found that for certain trace elements differences in the output did occur.

Most of the thermodynamic work carried out has used a basic system that consists of one trace element together with C, H, O, N, S and Cl at a pressure of 1 atm. In this review this basic system is referred to as the simple system. Where more or less complex systems have been investigated (that include more than one trace metal) the results from these studies are discussed. Key parameters for the thermodynamic studies carried out are given in Table 4.

An important parameter in these studies is the air to fuel ratio, indicated by the air excess number (λ). This is calculated by assuming that coal has the atomic composition given below and the stoichiometric reaction between coal and oxygen is described by the equation below,

$C_\alpha H_\beta S_\gamma N_\delta O_\varphi (H_2O)_\mu + (\alpha + \beta/4 + \gamma + \delta/2 - \varphi/2)O_2 \rightarrow \alpha CO_2 + (\beta/2 + \mu)H_2O + \gamma SO_2 + \delta NO$

The theoretical stoichiometric air requirement is $L_{min} = (\alpha + \beta/4 + \gamma + \delta/2 - \varphi/2)YO_2$ where YO_2 is the mole fraction of oxygen in air. If L is the real air supplied then $\lambda = L/L_{min}$. The implication of λ is summarised in Table 5 and the effect of λ varying on the behaviour of a number of elements is shown in Figure 9.

5.2.2. Review of elements

Arsenic (As)
Frandsen et al [27] found that in the simple system As was present as As_2S_2 up to 277°C† [27]. Between 277°C and 427°C As_4(g) was the major stable form of arsenic and above 427°C AsO(g) was the major stable form. In addition, between 277°C and 677°C As_2(g) was formed with a maximum occurrence at 477°C. Reed [28] found that for the temperature range of 430-930°C and pressure of 12.8atm that in the simple system with Ca and Fe that As_2(g) and As_4(g) were the dominant species but that AsO(g) was only a minor species. Overall Arsenic is predicted to be the gas phase above 277°C.

Reed [28] also looked at As without Fe and Ca but with Ni as it would be expected that the hot gas would see components that contained Ni. In this case As_2Ni_5 was predicted to be the only major species.

Barium (Ba)
In the temperature range 427°C to 827°C for the simple system with Ca $BaCl_2$ is the major species. At higher temperatures $BaCO_3$ and BaS become major species [28].

Boron (B)
For the simple system (without Ca) H_3BO_3(g) is the dominant species between 127°C and 627°C [27-28]. Above 627°C HBO_2(g) starts to form and becomes the dominant phase above 1027°C [27].

If Ca is included then at temperatures above approximately 527°C $Ca_3B_2O_6$ takes over from H_3BO_3(g) as the dominant species.

Beryllium (Be)
In the simple system BeO dominates below 677°C at 1atm [27] and 877°C at 12.8atm [28] (with Ca) with $Be(OH)_2$(g) dominating above these temperatures [27-28].

Cadmium (Cd)
Frandsen et al [27] found that in the simple system CdS is stable at temperatures up to 377°C. Above 377°C only Cd(g) is formed. No halides of cadmium are formed under reducing conditions. Similar behaviour was found by Reed [28] at 12.8atm (plus Ca) but with a changeover temperature of 467°C.

Cobalt (Co)
In the simple system including Ca and at 9.9atm Co_3S_4 was the major species in the range 427

† Temperatures have been converted where necessary to °C from K by subtracting 273. All species are condensed species apart from gaseous species that are denoted with (g).

to 627°C [28] but the thermodynamic data for this species was only valid up to 617°C. In addition the data for Co_9S_8 was only valid to 677°C. Omission of Co_3S_4 from the calculation gave Co_9S_8 [27] as the major species and omission of both gave Co [28]. Overall a condensed species will dominate.

Chromium (Cr)
In the simple system Cr_2O_3 was the stable form of chromium up to 1527K, where formation of CrO_2(g), CrO(g) and Cr(g) begins [27].

Copper (Cu)
In the simple system with Ca at 9.9atm Cu_2S is predicted to be the major species over the range 427 to 627°C [28].

Gallium (Ga)
In the simple system (no Cl) Ga_2S_3 dominates up to 357°C and Ga_2O_3 up to 727°C [27]. Above this the equilibrium chemistry becomes very complex with Ga_2S(g), Ga_2O(g), GaO(g) as well as Ga(g) occur in varying amounts. If Cl is included formation of GaCl(g) begins at 527°C at the expense of Ga_2S(g) and Ga_2O(g) and the amounts of Ga(g) produced at high temperatures are significantly decreased.

Germanium (Ge)
In the simple system GeO_2 is stable up to 427°C. Between 527°C and 1727°C the equilibrium form of Ge gradually changes with increasing temperature from GeS(g) to GeO(g) [27].

Mercury (Hg)
In the simple system Hg(g) is the dominant species above 57°C [28].

Manganese (Mn)
In the simple system at 9.9atm MnS dominates up to 957°C where MnO then dominates. If Ca is included this temperature is reduced to 797°C. $MnCl_2$(g) is the major gaseous species which only becomes significant at high temperatures and Cl levels [28].

Molybdenum (Mo)
In the simple system (with Ca) at 12.8atm MoS_2 is predicted to be dominant under most conditions with $CaMoO_4$ stable over a range of temperatures under certain conditions [28].

Nickel (Ni)
In the simple system NiS_2 dominates up to 147°C. Between 147°C and 277°C $NiS_{0.84}$ is the stable form of Ni. Above 277°C Ni_3S_2 is stable up to 772°C, where Ni is formed. Above 1427°C only Ni(g) and small amounts of NiO(g) are present in the system.

Phosphorus (P)
In the simple system H_3PO_4 is stable up to 157°C [27]. Between 157°C and 1127°C $(P_2O_3)_2$(g) is stable. Around 1077°C, formation of PO_2(g), PO(g) and PN(g) begins. The amounts of PO(g) and PO_2(g) increase continuously with increasing temperature above 1077°C.

Lead (Pb)
In the simple system (no Cl) PbS is stable up to 627°C with the formation of PbS(g) beginning at 477°C. The amount of PbS(g) reaches a maximum occurrence at 627°C and

decreases with increasing temperature above 627°C, mainly forming Pb(g). In addition, small amounts of PbO(g) are present above 1427°C. If chlorine is present, PbCl(g) is formed between 427°C and 1227°C with a maximum occurrence around 627°C.

Antimony (Sb)
In the simple system only SbS(g) is formed.

Selenium (Se)
In the simple system only $H_2Se(g)$ is formed. Note that gaseous carbonyl selenide, COSe(g), is not present in the database, DGFDBASE, used in this study, due to lack of thermochemical data.

Tin (Sn)
In the simple system SnO_2 is stable up to 377°C, where the formation of SnS(g) begins. SnS(g) is the major stable form of tin up to 1300K. Above 1027°C the equilibrium form of tin changes gradually with increasing temperature from SnS(g) to SnO(g). In addition, small amounts of Sn(g) are formed above 1427°C.

Titanium (Ti)
In the simple system with fluorine present TiF_3 is stable up to 79°C. Above 79°C only rutile is formed.

Vanadium (V)
In the simple system vanadium forms V_2O_3. Between 1227°C and 1477°C, the equilibrium form of vanadium changes from V_2O to $VO_2(g)$, the only stable form of vanadium above 1527°C.

Zinc (Zn)
In the simple system zinc is present as sphalerite, ZnS, up to 577°C, where the formation of Zn(g) begins. Above 727°C Zn(g) is the only zinc-containing chemical species.

5.2.3. Summary
Under the conditions considered the behaviour of the trace elements considered in the available literature are complex. A simple classification of the elements, as can be performed for the oxidizing conditions found in combustion systems, can not be carried out.

5.3. Cranfield University Thermodynamic Studies and Comparison with Available Literature

5.3.1. Introduction
Given the uncertainty and lack of reliable information in the literature, a thermodynamic study has been carried out to investigate the stability of potential product compounds in gasifier fuel gases. This study considered a number of variables:

- two gasifier processes: an oxygen blown entrained flow process (Prenflo) and an air blown fluidised bed process
- atmospheric and pressurised operation
- temperature ranges covering gasification and hot gas cleaning
- a range of sulphur and chlorine levels to cover the potential ranges of coal and coal/biomass fired systems

- the elements As, B, Ba, Be, Ca, Cd, Co, Cu, Hg, K, Mn, Mo, Na, Pb, Sb, Se, Sn, V, Zn

The elements Cr, Ni and Fe were not investigated as they are major alloying elements used in materials used throughout the fuel gas path and would be expected to be found on all component surfaces anyway.

5.3.2. Results

The results of this study are summarised in Tables 6-8. Table 6 indicates which elements are found in gasifier gases as mostly solids or gases throughout the temperature ranges considered (i.e. no phase changes in the major species) and whether process, gas pressure, sulphur or chlorine levels influenced any of the phase transitions found. Table 7 lists the major gas and condensed phases and the temperature ranges for these transitions. Finally, Table 8 groups the elements in terms of their 'volatility', i.e. in order of the transitions from gaseous to condensed phases. It should be noted that even elements with condensed phases could have significant vapour pressures.

Table 8 does not correspond with the frequently quoted three group classification of trace elements shown in Figure 8. This classification was originally developed for combustion systems and some reports directly translate this to gasification systems. As noted before [27-28] and found in this study, the same classification of elements is not applicable to combustion and gasification systems - there are several significant differences and indeed differences between gasification systems. This was also demonstrated by Lyyranen et al [29] as shown in Table 9.

Figures 10-15 illustrate the data generated during the thermochemical modelling and also highlight some of the pitfalls that exist. Figure 10 shows the effect of increasing the pressure on the potassium equilibrium diagram. The gas to solid transformation of the major species, KCl, is increased from ~700°C to ~900°C when the pressure increases from 1 to 20atm.

Figures 11 and 12 provide examples of how the data from some of these models can be greatly affected by the inclusion of another element. Figure 11 shows the effect of nickel on the equilibrium diagram for arsenic. As described above, nickel will be found throughout the hot gas path and its influence on the equilibrium models for other trace elements needs to be considered. Without the inclusion of nickel the arsenic data is comprised of gaseous species but with nickel present solid As_2Ni_5 is predicted to be the major species formed up to 1000°C. Figure 12 illustrates a similar situation, this time showing the effect of calcium on the boron equilibrium diagram. Additions of limestone or dolomite to the process provide a source of calcium and so with calcium present the boron data indicates the presence of a solid species.

Figures 13 - 15 show the effect of changing H_2S levels on the behaviour of zinc, tin and lead. These figures show that by reducing H_2S levels (the only change between the two conditions in each of these figures) dewpoints can be either lowered (e.g. zinc) or raised (e.g. tin), or different species made to dominate (e.g. lead).

5.3.3. Summary

Trace and alkali metals are more volatile in gasification systems and so the same broad classification of volatility used for combustion gases is not valid as different species are volatile. Sulphur and chlorine levels (both absolute and relative), as well as operating pressure and gasification process can influence the volatility of trace and alkali metal species. Hg, Pb, Zn, Cd, Se, Sb and Sn (and As, B and V in some systems) can pass through the gasifier

system, as well as alkali metals. Depending on the heat exchanger surface metal temperature Pb, Zn, Cd, Sn, Na, K potentially can condense onto the heat exchanger from the gas stream.

5.4. Comparison Of Thermodynamic Studies With Measured Trace Element Partitioning

5.4.1. Pilot Scale Fluidised Bed Gasifier Tests

A series of short (<12 hour) tests were carried out on the pilot scale fluidised bed gasifier, shown schematically in Figure 16. The aims of the tests were to investigate the composition and rates of formation of deposits on probes exposed at realistic heat exchanger operating temperatures to further validate the deposition model derived from the thermodynamic studies.

The coal used for the tests was Daw Mill: the proximate and ultimate analysis for the coal is given in Table 10. The gasifier operating conditions used for the tests are given in Table 11 and the typical raw fuel gas analysis is given in Table 12. Deposits were collected in the material testing zone from the gas stream at 700ºC on a probe held at a temperature of 400ºC (Figure 16), these conditions being typical of a gasifier heat exchanger.

The composition of the collected deposits were analysed using Energy Dispersive Spectroscopy (EDS); examples of the analysis data is shown in Figure 17. As described in section 5.3.3 sulphur and chlorine levels, as well as operating pressure and gasification process can influence the volatility of trace metal species. Potential trace species that could deposit on the probe in the gasifier tests are Pb, Zn, Cd and Sn. In the coal used, of these four elements, Zn is generally at the highest concentration followed by Pb, with Cd and Sn are at very low levels (<1ppm). The thermodynamics also favour Zn deposition over Pb as there is a greater thermodynamic driving force (Table 7). This is reflected in the results where Zn has deposited but none of the other elements have been found at levels detectable in a Scanning Electron Microscope/Energy Dispersive X-ray (SEM/EDX) analysis system (0.2 – 1 wt%). This result further validates the deposition model predicted by the thermodynamic studies.

5.4.2. Measured Trace Element Partitioning

When performing a comparison of the partitioning of trace elements measured in different studies there are a number of factors to be considered. Firstly, it would be expected that the partitioning behaviour is going to be dependent on fuel type, sorbents, additives, gasifier type, gas cleaning options and operating conditions. Secondly, the method and location used for sampling will be an important factor when dealing with very low concentrations of trace elements. Finally the method of quantitative chemical analysis can also give different results as found by Richaud et al [38]. Overall, considerable variability would be expected in the measured values and this has been seen with replicate tests within individual studies [28].

Figures 18 and 19 show measured trace element partitioning for an entrained flow gasifier with and without particle recycle. Partitioning data has also been reported by Reed [28]. This data compares well to the thermodynamic predictions in terms of volatility. Hg is predicted to be very volatile and to pass through the gasifier system and this has been found in the measurements. The predictions for B, Cd, Pb and Se are also fairly well reflected in the available partitioning data. Sb was predicted to be volatile but this is only reflected in Figure 18.

6. DOWNTIME CORROSION TESTING

Tests to investigate downtime corrosion (DTC) of materials in coal gasification environments have utilised different simulations of gasifier heat exchanger deposits (Table 3). These compositions have been produced by EPRI [21] and KEMA [22-23], from their experience of entrained gasification processes, and British Coal, from their experience of a fluidised bed partial gasifier [19, 23]. Other research laboratories have used these types of deposit composition in various downtime corrosion test programmes [e.g. 24]

6.1. Review of Previous Work

Research of downtime corrosion (DTC) testing in gasifier systems has been investigated using similar methods. Samples have sometimes been exposed to simulated gasifier environments at 550-600°C for up to 250 hours followed by exposure to a moisture-saturated atmosphere at 25-70°C for up to 250 hours [21, 23, 39-41]. The 'EPRI' test [21] has become the basis for most investigations and includes the coating (and subsequent re-coating) of the specimens with a simulated deposit (Table 3) during the test. Modifications to the test have been made by altering the composition of the simulated deposits (Table 3) to produce more realistic and/or aggressive simulated deposits by adding sulphide [14] or using $FeCl_3$ instead of $FeCl_2$ [24] or using char instead of slag (for ABGC systems). The $FeCl_3$ containing deposit was added prior to the high temperature cycle and so could be reduced to $FeCl_2$ but initially the deposit would be higher in chloride than the typical EPRI deposit. NPL [40] modified the test by withdrawing the samples to a cooler region of the furnace so a condensate (pH 1-3) would form on the samples. In the EPRI test dewpoint corrosion was avoided by inert gas flushing of the furnace during heating and cooling.

In terms of materials it is difficult to compare results as there is little overlap between studies and most test parameters vary. Some studies have indicated the effects of certain alloying elements [24, 39, 41] but work that has used a comprehensive number of materials can give the best indication of the effect of alloy composition. Simms et al [19] found that the ranking of the materials varied slightly between tests, but in general the trend in behaviour followed the ranking given by the pitting resistance equivalence number.

Where investigated, the least aggressive deposit was that consisting of char or slag alone [19, 21]. The chloride/char deposit caused more attack in most studies (although one study found the addition of chloride to have little effect [40]) but the chloride/sulphide/char deposit could be more aggressive [19]. A synergistic effect has been suggested for the combination of high and low temperature exposure cycles when compared to either cycle alone [19].

There have been few electrochemical studies of gasifier heat exchanger candidate materials in relation to downtime corrosion. One study [39] carried out an electrochemical evaluation to assess the passive behaviour of samples with and without scale. The sample scales were formed in a simulated gasifier environment at 600ºC for 100 hours and were anodically polarised in 0.5M NaCl solution at room temperature. It was found that the scaled samples did not show passive behaviour whilst the unscaled samples did. Tests were also carried out in 0.1M $K_2S_4O_6$ to investigate the influence of polythionic acid formation on downtime corrosion. It was concluded that the presence of polythionic acid could cause downtime corrosion in chloride free environments.

In general, electrochemical studies in aqueous chloride environments have studied stainless steels intended for use in chloride containing environments. For testing involving the gasifier heat exchanger materials, the test parameters have not been relevant to downtime testing and generally very simple test environments have been used. Overall, the data for all stainless steels do show trends that can indicate the effects of environmental conditions. The pitting resistance of stainless steels in aqueous environments generally reduces with increasing chloride concentration, decreasing pH and increasing temperature [44-45].

6.2. Downtime Corrosion Testing

Two types of testing have been carried out (electrochemical and DTC) using a range of candidate materials for gasifier heat exchangers.

6.2.1. Materials

The nominal compositions of the materials used in the work are given in Table 13 together with the corresponding pitting resistance equivalent number (PRENW (including tungsten)) as calculated from the equation below:

PRENW = %Cr + 3.3(%Mo + 0.5%W) + 16%N

It has been established that the pitting behaviour of stainless steels can be broadly related to composition using empirical relationships such as PREN. Crevice corrosion is influenced by many factors and therefore PREN is generally not so useful for prediction of this type of behaviour.

6.2.2. Electrochemical Tests

6.2.2.1. Experimental

Electrochemical testing using a triple electrode system (Figure 20) in naturally aerated solutions at 30°C has been used to measure the pitting potential, repassivation potential and hysteresis of the candidate materials. The test method is based upon ASTM G61 [46] with modifications for test solution and temperature. Electrochemical tests for pitting corrosion usually measure the pitting potential or the repassivation potential that either indicates the kinetics of nucleation or the kinetics of repassivation. Therefore neither potential relates to an incubation period or the propagation kinetics once initiation has occurred, so the DCT testing is required to gain this information. Nevertheless, these measurements provide a useful method for ranking the susceptibility of a set of materials in a given environment and to establish the aggressive species. Figure 21 shows a schematic representation of an anodic polarisation curve where the sample potential is increased and the resulting current measured. The flat region of fixed low current flow is where the material is passive (no significant corrosion), at the pitting potential (Enp) passivity is lost and with potential rise the current increases. If the polarisation is then reversed, the point at which the line crosses the passive region is the repassivation potential (Ecp). Enp, Ecp and the hysteresis in the loop created are a measure of pitting resistance and to some degree crevice resistance.

6.2.2.2. Results and Discussion

Electrochemical tests have been carried out in 1M NaCl and a NaCl/$FeCl_2$ solution at 30ºC to produce baseline data (Table 14). From these tests, the materials can be ranked in terms of pitting potential, repassivation potential and the hysteresis in the reverse sweep (i.e. difference

in Enp and Ecp). The values of these potentials and the resulting materials rankings are given in Tables 15 and 16, for the 1M NaCl and NaCl/$FeCl_2$ solutions respectively. The ranking of materials in this environment is generally the same for all three electrochemical measures and also matches the ranking found for the DTC test with the exception that IN625 could be separated from Haynes 556 as the best performer. Figure 22 shows typical potential versus current density data obtained for IN 625 and Alloy 800. The IN625 has a high pitting potential and almost no hysteresis in the repassivation loop. In contrast Alloy 800 has a much lower pitting potential and large hysteresis loop.

Figure 23 shows the potential versus current density data curve for T23 in 1M NaCl at 30ºC. This illustrates the completely different type of behaviour observed for this much lower alloyed steel.

6.2.3. Downtime Corrosion Tests

6.2.3.1. Experimental

DTC testing was carried out using a modified EPRI test. The apparatus used for this test work is illustrated in Figure 24. Specimens were coated with a deposit (deposit 1) consisting of 6.26% $FeCl_2$, 3.74% NaCl and 90% char (Tables 16-19). The composition (weight %) of the char was 56.48% carbon, 0.7% hydrogen, 0.46% nitrogen, 0.36% sulphur, 0.65% chlorine and 41.35% ash. Specimens were exposed to water saturated air at 30°C for 25 hour cycles initially. After exposure the deposit was removed and the specimens cleaned and examined before repeating the test. Longer cycles were also used to investigate whether the more resistant materials had an initiation period greater than 25 hours. Damage was assessed by visual inspection, weight loss and depth of attack (assessed using microscope technique) [47].

Weighing deposit samples in open glass containers before and after exposure gave the moisture content of the deposit after a continuous 75 hours exposure to the water-saturated environment. The average moisture contents for deposits 1 and 2 are given in Table 20. For deposit 1, the average moisture content of 0.63g per g of dry deposit equates to a chloride concentration of ~1M in the deposit in the DTC test and a pH of ~3 (from 1M chloride solution made from 6.26:3.74 $FeCl_2$/NaCl ratio but no char).

6.2.3.2. Results and Discussion

As the type and severity of attack on the materials tested varied significantly (Figure 25), a number of measurements have been used to quantify the degree of attack. Tables 21 and 22 summarise the type of attack and depth of attack and rank the materials as a result of these observations (Note AISI 310 is ranked lower than Haynes 160 and Sanicro 28 as it had many more pits). Only Alloy 800H and AISI 316 were severely attacked even after the first 25 hours as shown in Figure 25. The other materials showed little or no attack and no effect of increasing the test cycle time from 25 to 75 hours was evident. The degree of attack on AISI 316 and Alloy 800H was so great that weight loss has been used as a measure as shown in Figure 26. Alloy 800H was very severely attacked almost all over the exposed surface. A feature of the attack was that over intense areas of attack the deposit formed a hard crust.

The attack on the AISI 316 changed from an under-deposit/crevice type observed for periods of up to 50 hours to predominately pitting after longer exposures. This is apparent in Figure 26 where the weight loss curve after 50 hours becomes flatter, this being associated with the very local increase in size and depth of pits, which does not show up well in weight loss data.

The ranking of the overall resistance of the materials to the DTC test matches the PRENW ranking well (Tables 21 and 22).

7. DOWNTIME CORROSION AND PREVENTATIVE MEASURES

7.1. Introduction

Following a literature survey of the tests carried out elsewhere on downtime and dewpoint corrosion in gasifier heat exchangers, a detailed systematic approach to the test work was determined. The initial phase established the aggressive species in each of the environments to give a more fundamental understanding of the potential degradation mechanisms and provided a useful method for ranking the susceptibility of a set of materials in a given environment and to establish the aggressive species. Tests designed to replicate downtime conditions have been carried out based on the EPRI test for downtime corrosion with modifications based on the literature study and information gained from electrochemical testing. These more realistic tests have confirmed the relative significance of the different potential degradation mechanisms for the different candidate materials.

A series of tests assessed the effectiveness of candidate preventative measures against downtime corrosion. The candidate preventative measures include the use of dry atmosphere such as dry nitrogen, washing deposits off heat exchanger surfaces (with and without inhibitor) and mechanical removal of deposits. The majority of these tests have been carried out on clean samples, but one test was carried out using pre-oxidised/sulphidised samples.

7.2. Review of Downtime Preventative Measures

7.2.1. Overview

There are a number of methods that can be considered when attempting to reduce the corrosion rate in a given system and the most generally used are given below:

- Design
- Cathodic and Anodic Protection
- Pre-treatments
- Coatings
- Change Material
- Change Process Variables
- Condition Environment

Figure 27 shows simplified diagrams that demonstrates the two basic designs of heat exchanger. In Figure 27(a) the hot gas passes through a tube surrounded by water, in this case the deposit is formed on the inside of the tube. In Figure 27(b) water passes through a tube surrounded by hot gas, in this case the deposit is formed on the outside of the tube. Whether the deposit is on the inside or outside of the tube will not affect downtime corrosion. The main difference between the two designs in terms of this work will be the ease of application of preventative measures. There is little scope in altering the design of the system in a way that does not impact on the efficiency of the main function of the heat exchanger.

Cathodic and anodic protection both require a continuous electrolyte to be present which is clearly not viable. Pre-treatments for downtime corrosion resistance are unlikely to remain after operation of the heat exchanger at high temperature in the aggressive gasifier environment.

Using a more corrosion resistant material or corrosion resistant coating is clearly a viable option but would generally have a cost implication. The process variables are unlikely to be changed to produce a less aggressive deposit.

Therefore, from the list of options available, conditioning of the environment appears to be the most realistic method of corrosion reduction. This can be approached in three ways, firstly by changing temperature, secondly by reduction/removal of aggressive species in the local environment of the heat exchanger or finally by adding substances that reduce the corrosion attack i.e. inhibitors. These methods are discussed in more detail in sections 7.2.2 and 7.2.3.

7.2.2. Alteration of the Environment

A reduction in temperature generally has a significant effect in reducing corrosion rate. Cooling of the heat exchanger tubing relative to the local environment would produce enhanced condensation of moisture. Conversely reductions in corrosion rate can also be seen with increases in temperature in certain systems. Therefore, if the heat exchanger tubing was kept at say 50ºC or higher the absorption of moisture may be slowed or stopped. This is practical if the heat exchangers or local area are not undergoing maintenance.

Clearly keeping the deposits dry by using dry gas environment would be a solution but practically this does not seem viable. Also methods that reduce the chloride level and/or increase the local pH would be beneficial as both these factors are known to enhance initiation of crevice corrosion. Removal of the deposits by mechanical cleaning or water/steam blasting would remove or reduce the level of chloride. An alkaline water blasting solution would increase the local pH but potentially this could introduce species that are corrosive during high temperature operation.

7.2.3. Inhibitors

An inhibitor is a substance that is added in small concentrations to the environment and has the effect of decreasing the level of corrosion occurring. The use of an inhibitor would therefore not introduce large amounts of material into the gasifier system. There are many ways in which inhibitors have been classified; one such classification is given in Table 23. The selection of an inhibitor will be based on corrosion reduction achieved, ease of delivery into system and cost. Amongst the example species listed in Table 23 there are chemicals that are toxic and environmental hazards, so these factors will also need to be considered in the selection criteria.

7.3. Experimental

7.3.1. Materials

This activity used the same selection of materials, including those provided within the COST522 programme, that was used for the initial downtime test work, i.e. AISI 316L, AISI 310, AISI 347H, alloy 800, Sanicro 28, Haynes 160, Esshete 1250, Haynes 556, IN 625 and T23. The alloy compositions are given in Table 11.

7.3.2. Downtime Corrosion Test

The apparatus (Figure 24) and method used for this test was the same as detailed in section 6.2.3. The deposit used in this part, deposit 4, of the work consisted of 6.26% $FeCl_3$, 3.74% NaCl and 90% char (Tables 19). $FeCl_3$ was used in the place of $FeCl_2$ to produce a slightly

more aggressive deposit so that the reductions in corrosion damage caused by the preventative measures were more distinct. Damage was assessed by visual inspection, weight loss and depth of attack (assessed using microscope technique) [47].

Weighing deposit samples in open glass containers before and after exposure gave the moisture content of the deposit after a continuous 70 hours exposure to the water-saturated environment. The average moisture content for deposit 4 is given in Table 20. For deposit 3 the average moisture content of 0.70g per g of dry deposit equates to a chloride concentration of ~1.4M (and a lower pH value than deposit 1).

7.3.3. Downtime Corrosion Test with a Range of Deposit Thicknesses

7.3.3.1. Introduction

The aim of this test was to assess the effect of deposit thickness on the level of corrosion damage caused during downtime corrosion testing and indicate the possible beneficial effects of deposit removal. The test was carried out on one of the materials, AISI 347H, as this material was expected to show corrosion damage.

7.3.3.2. Experimental

Seven AISI 347H specimens were cleaned in 2-propanol and the surface area of the part of the specimen to be exposed was measured. Six specimens were then coated with a range of deposit thicknesses and the solvent evaporated off at 30ºC, deposit thicknesses ranged from 2 to 60mg/cm^2. All seven specimens were exposed to the downtime environment using the apparatus shown in Figure 2 for 90 hours at 30ºC. After exposure the specimens were ultrasonically cleaned in distilled water and rinsed with 2-propanol before drying. The specimens were then weighed and visually examined.

7.3.3.3. Results and Discussion

The first observation made was that the majority of the deposit washed off the samples very easily but where significant corrosion damage had occurred on the sample surface a thin hard black layer remained that was difficult to remove.

Photographs of three of the test specimens illustrating the type of damage caused are shown in Figure 28. For the thinnest deposit coatings the attack was mainly patches of small pits. For thicker deposit coatings the attack was mainly regions of metal loss and large round pits. The majority of the damage for the thicker deposits was found to be situated near to the edges. The specimen weight loss is plotted against the corresponding deposit thickness in Figure 29 and clearly shows that over the range of deposit thicknesses investigated that the damage on AISI 347H increases with increasing deposit thickness when exposed for 90 hours.

The chloride concentration produced by the deposit absorbing moisture would be the same for a thick or thin deposit. As the deposit is the only source of chloride ions the total chloride available will increase with deposit thickness. If chloride ions migrate to the specimen surface then a thicker deposit has the potential to produce a higher local chloride concentration. Also thicker deposits would be expected to form a better barrier to oxygen transport to the metal surface. Combined, these two factors should result in a thicker deposit having the potential to causing a faster breakdown of the metals passive film and a shorter incubation period. This suggests that removal of the majority of the deposit layer by mechanical cleaning would be beneficial.

7.3.4. Downtime Corrosion Test with Inhibitor

7.3.4.1. Experimental

The inhibitor chosen for the tests, thiourea, is used in pickling baths and has quoted efficiencies for similar aqueous environments in the 60-70% range (inhibitor efficiency (%) = $100(CR_{uninhibited} - CR_{inhibited}) / CR_{uninhibited}$ where CR = corrosion rate). Ideally the inhibitor used would have a higher efficiency but thiourea was readily available, works in acidic conditions and presents a low chemical hazard. A 1% (0.67g/L) solution of thiourea plus surfactant was used.

To provide data of corrosion rates without inhibitor deposit coated samples (deposit thickness of 3-4mg/cm^2) were exposed to DTC at 30ºC for 25 hour cycles for a total of 50 hours. The planned test time was 100 hours but the damage on some specimens after 50 hours was in danger of being out of range of the measurements on the optical microscope. After each cycle the samples were cleaned, dried and weighed, and an optical examination was carried out.

The inhibitor tests were carried out by adding a couple of drops of the inhibitor solution to the dry deposit (deposit thickness of 3-4mg/cm^2) before the samples were exposed to DTC. The test was carried out with 25 hour cycles for a total of 100 hours. After each cycle the samples were cleaned, dried and weighed, and an optical examination was carried out.

7.3.4.2. Results and Discussion

In this test the visual observations and measurements made on the optical microscope give the clearer picture of the effect of the inhibitor. The observations and measurements made for each material in the tests with and without inhibitor are given in Table 24, and it is clear that for materials with the smaller PRENW values the inhibitor has had a major effect. Corrosion damage still occurred but this was expected as the inhibitor used had a low efficiency. The T23 sample suffered severe general corrosion in both tests after just 25 hours. In the test with the inhibitor a 10% Inhibitor solution was used on the T23 sample for the second 25 hour cycle but this did not cause any reduction in corrosion. The weight change versus time graphs for these tests are shown in Figures 30 and 31. The results show that for the materials most likely to suffer downtime corrosion, the inhibitor used reduced the corrosion damage. The results also suggest that if an inhibitor with a much higher efficiency for the material and environment combination was used then the corrosion would be further reduced.

7.3.5. Effect of Inhibitor on Furnace Created Corrosion Products

7.3.5.1. Introduction

The aim of this part of the work was to test the effect of the inhibitor on samples with high temperature corrosion damage formed at 550ºC in a gasifier gas environment. It was decided that the best approach for this test was to expose the samples to the DTC test without applying simulated deposits for 4 cycles (total of 100 hours) and monitor the weight change. This would then be followed by another 4 cycles (without deposit) where the samples had been misted by an aqueous solution of the 1% thiourea inhibitor + surfactant solution prior to the start of each cycle. The effect of the inhibitor would be indicated in a change in the slope of the weight gain versus time curve.

7.3.5.2. Experimental

A sample from each material was placed into a furnace at 550ºC and exposed to the high H_2S containing gas (Table 25) used during this test programme for a continuous 248 hours and

then cooled to room temperature in nitrogen. The specimens were then put into the downtime corrosion test and exposed for 25 hour cycles for a total of 100 hours, with weights taken at each 25 hour interval after being dried for 1 hour at 50ºC. This was then repeated for a further 100 hours but with the samples being misted with the 1% thiourea + surfactant solution before each cycle.

7.3.5.3. Results and Discussion

Photographs of the specimens after the furnace exposure are shown in Figure 32. Corrosion scales are clearly visible on the specimens together with regions where this scale has spalled on a few specimens. The weight changes recorded were very small (less than 1mg change in 50 hours of exposure) and were thus very sensitive to any loss of deposits. Overall only one specimen, AISI 347H, gave significant results and for this material the inhibitor appeared to have no effect but weight gains were less than 0.3mg per 25 hours. It appears that the level of corrosion damage caused by the DTC test was too low for this test to give a clear indication of the effectiveness of the inhibitor. Figure 33 shows the specimens from Figure 32 after the 100 hours exposure to DTC plus 75 hours of DTC plus inhibitor. All of the specimens did show evidence of corrosion caused during DTC testing.

7.4. Proposed Corrosion Mechanism For Downtime Corrosion Testing

A proposed corrosion mechanism for the Downtime Corrosion Test is shown schematically in Figure 34. The mechanism is based on that proposed for crevice/under-deposit corrosion. Initially the corrosion reactions given below occur uniformly over the surface as shown in Figure 34(a).

Oxidation: $M \rightarrow M^{+} + e^{-}$

Reduction: $O_2 + 2H_2O + 4e^{-} \rightarrow 4OH^{-}$

The oxygen below the deposit layer is depleted due to the restricted oxygen transport through the deposit layer. Oxygen reduction ceases in these areas and dissolution of metal M occurs nearer to the deposit edge. This tends to produce an excess of positive charge that is balanced by the migration of chloride ions in the deposit towards the metal surface resulting in an increased local concentration of metal chloride. This metal chloride can be hydrolysed as shown in the equation below:

Hydrolysis: $MCl + H_2O \rightarrow MOH\downarrow + HCl$

This leads to the production of an insoluble metal hydroxide and increase in hydrogen ion concentration. The metal hydroxide forms a solid cap over the area of attack as shown in Figure 34(b).

8. SYNERGISTIC TESTING

8.1. Introduction

The conditions used for synergistic tests produced a range of simulated gasifier environments for a heat exchanger in an IGCC and ABGC system. For the IGCC system, the gas composition was chosen on the basis that it is an oxygen blown entrained flow gasifier with no sulphur removal prior to the heat exchanger. For an ABGC system, the gas composition

was chosen on the basis that it is an air-blown fluidised bed gasifier with in-bed sulphur retention.

Eight tests were carried out with the test parameters shown in the test matrix given in Table 26. Each of the eight tests started with a pair of specimens from the following alloys; AISI 316L, AISI 310, AISI 347H, Alloy 800, Sanicro 28, Haynes 160, Esshete 1250, Haynes 556, IN625 and T23 (total of 20 specimens in each test). Specimens were exposed for 7 x 100 hours at 450 or 550°C in either the high H_2S (= IGCC) or low H_2S (= ABGC) concentration simulated gases (compositions are given in Table 25) with and without the corresponding simulated deposit. For each test condition (i.e. gas / temperature combination) one of the pair of alloys were exposed to DTC for 25 hours at 30ºC.

8.2. Experimental

Specimens were cleaned, degreased and weighed before testing. The furnace arrangement used in these tests is shown in Figure 35. At the start of the test the furnace was flushed with nitrogen to remove the air before the test gas was added. The components of the test gas were supplied from two gas cylinders and mixed at the top of the furnace. The moisture was added to the High H_2S gas mixture by bubbling the gas from the hydrogen sulphide/carbon monoxide/carbon dioxide/methane/nitrogen cylinder through deionised water at the laboratory temperature. For the Low H_2S gas mixture moisture was added by bubbling the gas from the hydrogen sulphide/carbon monoxide cylinder through deionised water at 47°C. Prior to the furnace cooling at the end of the test it was again flushed with nitrogen to remove the test gas and avoid acid dewpoint corrosion.

Specimens tested with applied simulated deposits had the deposits applied before each HTGC cycle. Applying deposits during this part of the test had implications for the specimens that had DTC testing as applied deposits could fall off during the testing cycle before DTC testing. The main reason for applying the deposits before the HTGC cycle was to produce deposits for DTC testing that were as realistic as possible. The process of applying the deposits before DTC testing could have the undesirable effect of disrupting the corrosion layers produced during HTGC testing and additionally some alloys would suffer deposits/corrosion product loss during cooling in a real gasification system. The deposits were produced by mixing the dry deposit components together with propan-2-ol to produce a slurry. This slurry was applied to one side of the weighed test specimens and reweighed after the solvent had evaporated before testing. Deposits that corresponded with the process, and therefore gas, were used, the compositions are detailed in Table 19.

DTC testing was carried out as described in section 6.2.3.

The assessment of the corrosion damage on the test specimens involved a number of measurements and observations. The weight change data recorded during these tests could not be used as the primary measure of corrosion damage as the following factors demonstrate.

1. Samples were not in crucibles during testing so spalled corrosion product and/or deposit was not measurable.
2. Samples were only deposit coated on one side so the weight change would include both coated and uncoated areas.
3. The application of deposits can disturb/remove previously applied deposits and corrosion product.

Therefore the primary measurement of HTGC damage was optical measurements of oxide and sulphide thicknesses (maximum and typical) on sample cross sections to assess metal damage and allow comparisons to be made. Photographs were taken of the cross section features to show the effects of DTC.

8.3. Results and Discussion

The data generated from these tests are complex to analyse so to aid in the analysis a material selection failure criterion based on high temperature corrosion rate has been applied. The use of sulphide thickness measurements is unreliable as the sulphide is often combined with the applied simulated deposit and in many cases had detached from the specimen surface. Typical and maximum oxide thicknesses have therefore been used in a very simple failure model.

If the following assumptions are made for example

- oxide thickness equals metal loss
- a corrosion allowance of 2.5mm
- 10 year life
- linear corrosion rate

then the maximum oxide thickness allowable in the 700 hour HTGC tests is 20μm.

Figures 36-43 show bar charts of the maximum oxide measurements made for each test and each figure compares the results for each material with and without DTC. The oxide data has been used together with the failure criterion of 20μm to generate summary tables of the performance of the alloys tested under each test condition (Tables 27 and 28).

Photographs of the major cross-section features are shown in Figures 44-58.

8.3.1. AISI 316L, AISI 310, AISI 347 and Esshete 1250

These alloys showed similar behaviour in the tests. Using the 20μm failure criterion described above the performance (typical oxide) of these alloys in the high H_2S gas was borderline at 450˚C and poor at 550˚C. In the low H_2S whilst the HTGC performance (oxide thickness) was good the DTC performance was poor. The effects of DTC testing were always more apparent in tests where HTGC performance was good. For example, in Figure 51 AISI 347 tested in low H_2S gas at 450˚C displays major DTC damage with and without applied deposits.

In the low H_2S gas Esshete 1250 at 450ºC demonstrates pitting due to DTC with and without deposits (Figure 57). In the same gas both AISI 316 and AISI 310 at 550ºC with deposits show damage due to DTC (Figures 48 and 50 respectively). Overall AISI 347 and Esshete 1250 would not be recommended for use as a gasifier heat exchanger material at 450ºC in either gas. AISI 316 and AISI 310 would only be considered for use at 450ºC in the low H_2S gas.

8.3.2. Alloy 800

Alloy 800 showed good high temperature performance in the low H_2S gas at 450 and 550˚C. In the high H_2S gas the performance was poor at 450˚C with applied deposits and at 550˚C. In this gas the inclusion of a DTC test has the effect of considerably increasing the oxide thickness on deposit coated specimens compared to the tests without DTC testing. This is not seen in the absence of deposit.

At 450˚C in the high H_2S gas with and without deposits the specimens with the DTC test display intergranular attack with oxide forming within these regions of attack (Figure 44). At 550˚C in the same gas the intergranular damage is not seen as the damage from HTGC dominates (Figure 45) although some intergranular damage was seen at the specimen edges (Figure 45). In the low H_2S gas at 550ºC in the test with applied deposits and DTC there is massive pitting damage (Figure 46). Overall Alloy 800 appears only to be suitable for use at 450ºC in the low H_2S gas.

8.3.3. Sanicro 28, HR 160 and Haynes 556

These three materials showed the best performance. All performed well in both high and low H_2S gas at 450˚C and at 550˚C in the low H_2S gas. The performance at 550˚C in the high H_2S gas was mixed but still was superior to the other alloys tested. Overall the best alloy in terms of HTGC performance was HR 160 but when alloy cost is considered the lower cost of Sanicro 28 compared to the small increase in performance that HR 160 offers means that Sanicro 28 appears to be the best choice.

8.3.4. IN 625

IN 625 showed HTGC performance that was no better than AISI 310 but appeared to have better resistance to DTC as predicted in the DTC tests (section 6.2). Less expensive alloys offer better performance than IN 625.

8.3.5. T23

The performance of the T23 was very poor in all tests. During testing the corrosion and deposit layer spalled resulting in cross sections with no visible corrosion layers (Figure 55). This alloy would not be recommended to be used for a gasifier heat exchanger at 450 or 550ºC.

9. IDENTIFICATION OF SAFE OPERATING WINDOWS

The effects of two simulated gasifier environments (IGCC and ABGC gasifier systems) on the life of candidate heat exchanger materials have been investigated. The IGCC system is based on an oxygen blown entrained flow gasifier with no sulphur removal prior to the heat exchanger. The ABGC system is based on an air-blown fluidised bed gasifier with in-bed sulphur retention. Detailed results for the HTGC and DTC performance of the candidate materials have been given in sections 6-8. To allow easier interpretation of the results generated by this project summary materials degradation maps can be produced. An example map, based on data from Table 28, is given in Figure 59. Most of the alloys tested in the ABGC environment (= low H_2S) in the range of 450 - 550ºC had adequate high temperature resistance to be considered for construction of a heat exchanger. In these conditions a number of the alloys were more likely to fail due to DTC damage and therefore the presence and composition of deposits is a major factor.

The IGCC environment (= high H_2S) was more aggressive than the ABGC environment as would be expected with the higher H_2S level. At 450ºC there are still a number of alloys that give satisfactory performance even in the presence of deposits. At 550ºC most of the alloys can not be considered due to poor HTGC performance and even the best performing alloys are borderline in terms of HTGC and DTC performance. In terms of cost and overall performance Sanicro 28 is clearly the best candidate material investigated in this study.

10. CONCLUSIONS

This project has investigated a range of material performance and selection issues associated with the formation of deposits in gasifier heat exchangers.

A literature review of the formation of deposits on gasifier heat exchangers has been carried out. This considered a range of gasification processes, mechanisms by which deposits can form on evaporator and superheater surfaces in these environments and the potential effects of such deposits. A search has been carried out for heat exchanger deposit compositions reported in the literature. In light of the limited information available, and the high levels of trace elements reported in gasifier deposits, this review was extended to cover the fate of trace element species in gasifier fuel gases. Again, only a limited literature exists on this subject (in contrast to a large literature base for combustion gases). An additional thermodynamic study was carried out at Cranfield University to fill in some of the gaps that obviously existed in the literature. These thermodynamic predictions were compared to reported distributions of trace elements through gasifier hot gas paths

All the data gathered, from theoretical studies and plant observations, indicate that trace element partitioning between condensed and vapour phases is significantly different in gasification and combustion systems. The same broad classification of trace element volatility produced for combustion gases is not applicable to gasifier fuel gases, and indeed there can be significant differences between gasification processes. In all gasification systems, many more trace elements are volatile and many have the potential to be transported along the fuel gas path (usually as chlorides) and condense onto heat exchanger surfaces (as chlorides or sulphides). Plant observation of significant levels of Pb, Zn, As, Cd, Se, Sb and Ge on heat exchanger surfaces confirms these predictions. Important parameters that affect the behaviour of trace elements in the fuel gas paths have been highlighted as: sulphur and chlorine levels (both absolute and relative); operating pressure; gasification process. Other components in the deposit result from deposition of particles derived from the fuel mineral matter and unburnt carbon. Heat exchanger design will have a significant effect on the formation of deposits by a combination of condensation and the various potential particle deposition mechanisms, due to differences in gas flows and gas/surface temperatures.

Electrochemical tests have been carried out to produce baseline data for the candidate heat exchanger materials which were then ranked in terms of predicted DTC resistance. The EPRI DTC test has been modified to more accurately simulate real deposits observed in service. Alloy ranking given by this DTC test and electrochemical studies have shown a strong correlation with that predicted by PRENW. Alloy 800 and AISI 316 showed very poor corrosion resistance in the DTC test. IN625 demonstrated the greatest resistance to the electrochemistry test.

The effectiveness of candidate preventative measures against downtime corrosion have been assessed. Tests have shown that for simulated deposits applied to clean specimens that mechanical removal of deposits and/or washing deposits off heat exchanger surfaces will reduce corrosion rates. The addition of an inhibitor to the wash solution would further reduce corrosion. The DTC test using an inhibitor (without applied simulated deposits) carried out on samples pre-oxidised/sulphidised at 550ºC for 248 hours in a gasifier gas was inconclusive in the time available.

Synergistic tests have been carried out in a range of simulated gasifier environments for a heat exchanger in an IGCC and ABGC system. For the IGCC system, the gas composition was chosen on the basis that it is an oxygen blown entrained flow gasifier with no sulphur removal prior to the heat exchanger. For the ABGC system, the gas composition has been chosen on the basis that it is an air-blown fluidised bed gasifier with in-bed sulphur retention. The synergistic degradation test work involved exposing deposit-coated samples to (i) high temperature gaseous corrosion with 100 hour thermal cycles and (ii) alternating periods of high temperature gaseous corrosion (100 hours) and downtime (25 hour). Exposures in the gaseous environments were carried out at 450 and 550°C. Sanicro 28, HR 160 and Haynes 556 were found to give the best performance over all the conditions tested.

The data generated has been used to identify safe operating windows where factors do not combine to produce rapid heat exchanger failures. Aspects such as candidate heat exchanger materials, gasifier type, fuel and fuel gas compositions, deposit compositions and heat exchanger operating conditions have been investigated.

11. FURTHER WORK

The test programme has demonstrated that gasifier hot gas path environments are potentially very aggressive for materials both during plant operation and off-line periods. Current materials are restricted to modest steam conditions and are not suitable for use as superheaters with commercially viable lives. However, many gasification cycles would be more efficient if at least some superheating could be carried out by the fuel gas heat exchanger. Alloy research and development is required to produce materials with extended lives at temperatures below 450ºC and viable service lives at temperatures above 450ºC. As well as alloy development the use of coatings and/or co-extruded heat exchanger tubing may provide a route to achieve this target. This research area would also require investigation of the weldability of the new materials/coatings and the resulting mechanical properties, strength, high temperature corrosion-fatigue etc., in the parent material and weld region.

12. REFERENCES

1. Takematsu T and Maude CW (1991) – 'Coal gasification for IGCC power generation' IEACR/37, London, UK, IEA Coal Research.
2. Liere J Van and Bakker WT (1993) – 'Coal gasification for electric power generation' Materials at High Temperature 11 (1-4) pp4-9.
3. Mendez-Vigo I, Chamberlain J and Pisa J (1997) – 'ELCOGAS IGCC plant in Puertollano, Spain' Materials at High Temperature 14 (2/3) pp15-20.
4. Blough JL and Roberson A (1993) – 'Pressurized fluidized bed combustor system' Materials at High Temperature 11 (1-4) pp10-14.
5. Stambler I (1993) – Gas Turbine World 23 pp22-27.
6. Stringer J and Wright IG (1995) – 'Current limitations of high-temperature alloys in practical applications' Oxidation of Metals 44 (1/2) pp265-308.
7. Bakker WT (1995) – 'Mixed oxidant corrosion in non-equilibrium syngas at 540°C' EPRI Report TR-104228, March 1995.
8. Lloyd DM (1989) – Research and Development of high Temperature Materials for Industry, Ed. Bullock E, Elsevier, pp339-359.
9. Stringer J (1984) – High Temperature Materials Corrosion In Coal Gasification Atmospheres, Ed. Norton J, Elsevier.
10. Gesmundo F (1990) – High Temperature Materials for Power Engineering, Eds. Bachelet et al, Kluwer.
11. Gesmundo F (1991) – Advanced Materials for Power Engineering Components: The Corrosion of Metallic Materials in Coal Gasification Atmospheres – Analysis of Data from Cost 501 (round 1) Gasification Subgroup. EUCO/MCS/08/1991.
12. Bakker WT (1987) – Proceedings of Seventh EPRI Annual Conference on Coal Gasification, EPRI, Palo Alto, Calirornia, USA.
13. Proceedings First International Workshop on Materials for Coal Gasification Power Plant, Petten, The Netherlands, June 1993. Materials at High Temperature 11 (1993)
14. Erosion/Corrosion of Advanced Materials for Coal-Fired Combined Cycle Power Generation, Final and Summary Reports on JOUF-0022 (1994)
15. Kristiansen A (1996) – 'Understanding coal gasification' IEACR/86 March 1996, IEA Coal Research, London,
16. Clarke LB and Sloss LL (1992) – 'Trace elements – emissions from coal combustion and gasification' IEA Coal Research, London, Report No. IEACR/49.
17. Gupta R, Wall T and Baxter L (eds.) (1999) – 'Impact of mineral impurities in solid fuel combustion' Proceedings of an Engineering Foundation Conference on Mineral Matter in Fuels, 2-7 November 1997, Kailua Kona, Hawaii, Pubs,. KluwerAcademic/Plenum Publishers, New York.
18. Oakey JE and Simms NJ (1998) – 'Materials requirements for advanced coal fired power generation technologies' In Proceedings of the 6th Liege Conference on Materials for Advanced Power Engineering 1988, Part II. Eds. Lecomte-Beckers J, Schubert F and Ennis PJ, pp651-662.
19. Simms NJ, Lowe TM, Scott INS and Oakey JE (1997) – 'Materials for gasifier hot gas path components in advanced combined cycle power plants' Final Report No R106 UK Cleaner Coal Technology Programme 1997.
20. Bakker WT (1993) – 'Effect of gasifier environment on materials performance' Materials at High Temperature 11 (1-4) pp81-89.
21. Perkins RA, Marsh DL and Sarossiek AM (1988) – 'Downtime corrosion in syngas coolers of entrained slagging gasifiers' EPRI Report AP5996.

22. Huijbregts WMM, Kokmeijer E and Zuilen HG van (1993) – 'Sulfidation, down-time corrosion and corrosion-assisted cracking on high alloy materials in synthetic coal gasifier environments' Materials at High Temperature 11 (1-4) pp58-64.
23. Simms NJ, Bregani F, Huijbregts WMM, Kokmeijer E and Oakey JE – 'Coal gasification for power generation: materials studies' In Proceedings of the 6th Liege Conference on Materials for Advanced Power Engineering 1988, Part II. Eds. Lecomte-Beckers J, Schubert F and Ennis PJ, pp663-679.
24. Norton JF, Bakker WT and Maier M (1999) – 'Corrosion of heat exchanger alloys exposed to a non-equilibrated co-based sulfidizing environment at 550°C' Paper 99069 NACE/99, San Antonio, Texas, April 1999.
25. Morgantown Energy Technology Center Report (1989) – 'Vaporization of trace element species from coal under gasification and combustion conditions' US Department of Energy, Morgantown, West Virginia
26. Mojtahedi W (1989) – 'Trace metal volatilisation in fluidised-bed combustion and gasification of coal' Combustion Science and technology 63 pp209-227
27. Frandsen F, Dam-Johansen K & Rasmussen P (1994) - 'Trace Elements from Combustion and Gasification of Coal-an Equilibrium Approach' Progress in Energy and Combustion Science 20 (2) pp115-138
28. Reed GP (2000) – 'Control of trace elements in gasification' PhD Thesis, Imperial College.
29. Lyyränen J, Jokiniemi J, Mojtahedi W and Koskinen J (1995) – 'Equilibrium modelling of trace element behaviour in fluidized bed combustion and gasification of coal' Journal of Aerosol Science 26 ppS687-S688.
30. Helble JJ, Mojtahedi W, Lyyränen J, Jokiniemi J and Kauppinen E (1996) – 'Trace element partitioning during coal gasification' Fuel 75 (8) pp931-939.
31. Norman J, Pourkashanian M and Williams A (1997) – 'Modelling the formation and emission of environmentally unfriendly coal species in some gasification processes' Fuel 76 (13) pp1201-1216
32. Hurley JP, Nowok JW and Kuhnel V (1999) – ' Modeling of Ni, Ge and Pb speciation in coal gasification systems' Proceedings 13th Annual Fossil Energy Materials Conference, Knoxville, Tennessee, May 1999.
33. Yan R, Gauthier D and Flamant G (2000) – 'Possible interactions between As, Se, and Hg during coal combustion' Combustion and Flame 120 (1-2) pp49-60
34. Yan R, Gauthier D, Flamant G and Badie JM (1999) – 'Thermodynamic study of the behaviour of minor coal elements and their affinities to sulphur during coal combustion' Fuel 78 (15) pp1817-1829.
35. Salo K and Mojtahedi W (1998) – 'Fate of alkali and trace metals in biomass gasification' Biomass and Bioenergy 15 (3) pp263-267
36. Clarke LB (1993) – 'The fate of trace elements during coal combustion and gasification' Fuel 72 (6) pp731-735
37. Frandsen F, Erickson TA, Kuhnel V, Helbe JJ, Linak WP (1996) – 'Equilibrium Speciation of As, Cd, Cr, Hg, Ni, Pb, and Se in Oxidative Thermal Conversion of Coal - A Comparison of Thermodynamic Packages' In Proceedings of 3rd International Symposium on Gas Cleaning at High Temperatures, Karlsruhe, Germany pp462-473.
38. Richaud R, Lachas H, Healey AE, Reed GP, Haines J, Jarvis KE, Herod AA, Dugwell DR and Kandiyoti R (2000) – 'Trace element analysis of gasification plant samples by icp–ms: validation by comparison of results from two laboratories' Fuel 79 (9) pp1077-1087.
39. Kihara S, Nakagawa K, Ohtomo A, Kato M (1987) – 'Corrosion resistance of high-chromium steels in coal gasification atmospheres' Materials Performance 26 (6) pp 9-17

40. Saunders SRJ, Gohil DD and Osgerby S (1997) – 'The combined effects of downtime corrosion and sulphidation on the degradation of commercial alloys' Second International Workshop on Corrosion in Advanced Power Plants, Tampa, Florida, USA, 3-5 March 1997, Materials at High Temperatures 14 (3) pp237-243
41. Norton JF, Maier M and Bakker WT (1997) – 'Corrosion of 12% Cr alloys with varying Si contents in a simulated dry-feed entrained slagging gasifier environment' Second International Workshop on Corrosion in Advanced Power Plants, Tampa, Florida, USA, 3-5 March 1997, Materials at High Temperatures 14 (2) pp81-91.
42. Simms NJ, Nicholls JR and Oakey JE (2001) – 'Materials Performance in Solid Fuel Gasification Systems' Materials Science Forum, 369-372 pp947-954.
43. John RC, Fort WC and Tait RA (1993) - Materials at High Temperature, 11 pp124-132.
44. Oldfield JW (1987) – 'Test techniques for pitting and crevice corrosion of stainless steels and nickel-base alloys in chloride-containing environments' International Materials Reviews 32 (3).
45. Haynes AG (1992) – 'Duplex and high alloy corrosion resisting steels' Lloyd's Register Technical Association, London.
46. ASTM G61 - Standard Practice for 'Conducting Cyclic Potentiodynamic Polarization Measurements for Localized Corrosion'
47. ASTM G46 – Standard Practice for 'Examination and Evaluation of Pitting Corrosion'
48. Clubley BG (Ed.) – 'Chemical Inhibitors for Corrosion Control' Proceedings of an International Symposium, 21-22 April 1988. The Royal Society of Chemistry (1990).

Table 1. Gasifier Gas Compositions

Gas Species	Units	Oxygen Blown Gasifiers			Air Blown Gasifier Fluidised Bed
		Entrained Slagging		Fluidised Bed	
		Dry Feed	Slurry Feed		
CO	%	62 – 64	35 – 45	30 – 40	15 – 20
CO_2	%	2 – 4	10 – 15	10 – 15	5 – 8
H_2	%	27 – 30	27 – 30	24 – 28	10 – 15
H_2O	%	0 – 3	15 – 25	11 – 20	5 – 12
N_2	%	1 – 5	0 – 2	0 – 2	40 – 50
CH_4	%	n/a	n/a	3.5	2 – 4
H_2S *	vppm	2000 – 12000	2000 – 12000	2000 – 12000	300 – 5000
NH_3	vppm	200 – 500	2000 – 5000	200 – 500	500 – 1500
HCl *	vppm	50 – 1000	50 – 1000	50 – 1000	50 – 500

* Dependent on coal Sulphur and Chlorine content

Table 2. ABGC Deposit Analysis for Cooled Probe Upstream of Filter Unit [19]

Crystalline phases (by XRD)	
Major	SiO_2, CaO, CaS, $CaCO_3$, $CaSO_4$, $CaSO_4.2H_2O$, NH_4Cl
Minor	$(Ca, Na)(Si, Al)_4O_8$, FeS, PbS, ZnS, $PbSO_3$, $ZnSO_4$
Elements (by EDX)	
Major	C, Al, Si, Ca, S, O
Minor	Pb, Zn

Table 3. Deposit Compositions Used in Literature Downtime Corrosion Testing.

	Composition (weight %)								
	EPRI [21]		KEMA [1] [22]	NPL [40]		Simms et al [19]			Norton et al [24,41]
Component	1	2		1	2	1	2	3	
Slag	100	90	Yes	-	-	-	-	-	80
Char	-	-	-	100	90	100	90	90	-
Carbon	-	-	-	-	-	-	-	-	10
NaCl	-	3.74	37.4	-	3.74	-	3.74	2	5
KCl	-	-	-	-	-	-	-	1	-
PbS	-	-	-	-	-	-	-	4	-
ZnS	-	-	-	-	-	-	-	1	-
$FeCl_2$	-	6.26	62.6	-	6.26	-	6.26	2	-
$FeCl_3$	-	-	-	-	-	-	-	-	5

[1] Ratio of fly ash to eutectic salt mix not specified

Table 4. Scope of Work Reported in Literature. T1 and T2 Indicate Temperature Range of Study in °C. P1 and P2 Indicate Pressures Investigated in atm, λ is Air Excess Number. NS = Not Stated. (*Modified Version)

Ref	Program	Database	T_1	T_2	P_1	P_2	λ	Fuel
25	SRI*	In-house	27	1527	1	-	NS	Wyodak coal
26	NS	JANEF	200	1200	1.01	10.1	0.5	High (4.7%) & low S (1.1%) coal
27	MINGTSYS	DGFDBASE	77	1727	1	-	0.6	Subbituminous coal
28	MTDATA	SGTE	427	977	9.9	12.8	NS	Daw Mill coal
29	ChemSage	NS	380	1380	11.9	19.7	0.53	Coal (λ=0.9 was used for P1)
30	ChemSage	NS	27	1527	1	20	?	Illinois No 6 coal
31	Equitherm	Equitherm	NS	NS	NS	NS	NS	NS
32	FACT	NS	NS	NS	NS	NS	NS	NS
33	SOLGAMIX	GFEDBASE	127	1527	1	-	0.6	Bituminous coal
34	ALEX	JANAF	127	1727	1	-	0.6	High & low ash bituminous coals

Table 5. Summary of Air Excess Numbers (λ) Values.

$\lambda=0$	Absence of oxygen
$0<\lambda<1$	Oxygen deficient (reducing)
$\lambda\approx1$	Close to stoichiometric
$\lambda>1$	Oxygen rich (oxidising)

Table 6. Summary of Predicted Fate of Trace and Alkali Metal Species in Gasification Gases (including their sensitivity to process conditions) ✔ = yes, X = no, **S = under some P, Cl, S conditions; - = not applicable; ( ) = under some conditions.**

Element	Majority species always in vapour phase		Majority species always in solid phase		gas→solid transformation sensitivity			
	ABGC	Prenflo	ABGC	Prenflo	Pressure	Cl	S	Process
As	✔	✔	X	X	-	-	-	-
As (+Ni)	X	X	S	S	✔	✔	✔	(✔)
B	✔	✔	X	X	-	-	-	-
B (+Ca)	X	-	X	-	X	X	X	✔
Ba	X	X	S	-	✔	✔	✔	✔
Be	X	X	X	X	X	X	X	X
Ca	X	X	S	S	(✔)	(✔)	(✔)	(✔)
Cd	S	S	X	X	✔	✔	✔	X
Co	X	X	S	X	✔	✔	✔	(✔)
Cu	X	X	X	X	(✔)	✔	✔	(✔)
Hg	✔	✔	X	X	-	-	-	-
K	X	X	X	X	✔	✔	✔	(✔)
Mn	X	X	S	X	X	✔	✔	(✔)
Mo	X	X	S	X	(✔)	✔	✔	(✔)
Na	X	X	X	X	✔	✔	✔	(✔)
Pb	S	S	X	X	X	✔	✔	X
Sb	✔	✔	X	X	-	-	-	-
Se	✔	✔	X	X	-	-	-	-
Sn	S	S	X	X	X	✔	✔	X
V	X	✔	✔	X	-	-	-	-
Zn	S	?	X	X	X	✔	✔	X

Table 7. Summary of Behaviour of Trace and Alkali Metal Species in Gasifier Gases in Terms of Major Gaseous and Solid Species as well as Gas → Solid Transformation Temperature Ranges Indicated by Thermodynamic Study, ( ) = Prenflo only.

Element	Major Gas Species	Major Solid Species	Gas → Solid Transformation Temperature Range (°C)
As	As, As_2, As_4, AsS	-	-
As (+Ni)	AsS (As)	As_2Ni_5, As_8Ni_{11}	1020-1460
B	BHO_2, $B(OH)_3$	-	-
B (+Ca)	$B(OH)_3$ (BHO_2)	$B_2Ca_3O_6$	solid→gas 420-840
Ba	$BaCl_2$, BaClHO	$BaCl_2$, BaS, $BaCO_3$	900-1040 (or >1200)
Be	BeH_2O_2	BeO	840-960
Ca	-	$CaCl_2$, CaS, $CaCO_3$	-
Cd	Cd, $CdCl_2$	CdS	400-540 (or <400)
Co	$CoCl_2$ (Co)	Co, Co_9S_8	600-1340
Cu	CuCl, Cu_3Cl_3, (Cu, CuH)	Cu, Cu_2S	520-960
Hg	Hg	-	-
K	KCl, K_2Cl_2	KCl	700-900
Mn	$MnCl_2$ (MnCl)	MnO, MnS	440-1260
Mo	$MoClO_2$, $MoCl_2O$, $MoCl_2O_2$, $MoHO_2$)	MoS_2	700-1200
Na	NaCl, Na_2Cl_2	NaCl	670-900
Pb	Pb, PbCl, $PbCl_2$ PbS	Pb, PbS	560-640 (or <400)
Sb	SbCl (Sb)	-	-
Se	SeH_2 (SeH)	-	-
Sn	SnS, $SnCl_2$	SnO_2, SnS	460-560 (or <400)
V	(VCl_2, VCl_3, $VOCl_3$)	V_2O_3	-
Zn	Zn, $ZnCl_2$	ZnS	460-780

Table 8. Summary of Predicted Volatility of Trace and Alkali Metals in Gasification Gases from Our Thermodynamic Study, ( ) = significant differences in behaviour predicted for different gas conditions

Increasing Volatility	Element
⇧	B, Hg, Sb, Se (As, V)
	Cd, Pb, Sn, Zn (As, B)
	Co, Cu, K, Mn, Mo, Na
	As, Ba, Be
	Ca (V, As, B)

Table 9. Classification of Trace Elements Based on Volatility for Two Pressurized Gasification Conditions [29].

Volatility	12 bar, λ = 0.9	20 bar, λ = 0.53
Highly volatile	As, Hg, Sb	As, Hg, Sb, Se
Volatile	Cd, Pb, Sn	Cd, Pb, Zn
Slightly volatile	Cr, Cu, Ni	Be, Cu, Mo
Not volatile	Co, Mn, Ti, V	Cr, Co, Mn, Ni, V

Table 10. Proximate and Ultimate Analysis of Daw Mill Coal Used in Pilot Scale Fluidised Bed Gasifier Tests

Proximate analysis	% ad	Ultimate analysis	%
Moisture	6.1	C (dmmf)	81.3
Ash	4.4	H (dmmf)	4.8
Volatile matter	35.7	O (dmmf)	11.5
Fixed carbon	53.8	N (dmmf)	1.28
Volatile matter (dmmf)	40.4	Organic sulphur (db)	1.12
		Sulphate as S (db)	0.1
		Pyritic Sulphur (db)	0.28
		Cl (db)	0.21
		CO_2 (db)	0.45

Table 11. Operating Conditions for Pilot Scale Fluidised Bed Gasifier (0.15m) Tests.

Feedstock	Bituminous Coal (3.5 mm)
Coal Feed Rate	Typically 5 kg/hr
C:O ratio	2.5
Bed Temperature	980 ˚ C
Bed Height (fluidised)	0.6 m
Gas velocity	1 m/s
Fluidising gas	air
Bed Off-take	1 kg/hr
Air preheated	300 ˚C

Table 12. Typical Raw Gas Concentrations Obtained with the Pilot Scale Fluidised Bed Gasifier with Bed Temperature of 980 °C

Gas	% (volume)
H_2	4.28
CO	5.05
CH_4	0.77
CO_2	4.82
H_2S	0.04

Table 13. Compositions of Alloys [PRENW =%Cr+3.3(%Mo+0.5%W)+16%N]

Alloy	Composition (wt %)					PREN W
	Cr	Ni	Fe	Mo	Others	
Alloy 800H	21	32	Bal		0.75Mn	21.0
AISI 316L	16.8	11.2	Bal	2.3	1.5Mn	24.0
AISI 310	25	20	Bal		1.5Mn 1.5Si	25.0
Haynes 160	28	Bal.	3.5	1.0	0.5Mn 30Co 2.7Si 1W	29.7
Haynes 556	21.6	19.9	Bal.	2.8	18Co 2.4W 0.2N	38.0
Sanicro 28	27	31	Bal.	3.5	2Mn	38.6
IN 625	21.5	Bal.	2.5	9.0	0.5 Mn	51.2

Table 14. Composition of Solutions used for Electrochemistry Tests

Solution	Concentration (g/L)		Chloride concentration (moles)	Approx. pH
	NaCl	$FeCl_2$		
1M NaCl	58.44	-	1	5
$NaCl/FeCl_2$	23.08	38.64	1	3

Table 15. Pitting Potential, Repassivation Potential and Hysteresis in Reverse Polarisation Results for Materials in 1M NaCl at 30ºC.

Alloy	E_{np} (mV(SCE))	E_{cp}(mV(SCE))	E_{cp}- E_{cp} (mV)	Rank
Alloy 800H	107	-200	307	6
AISI 316L	158	-100	258	5
AISI 310	175	-33	208	4
Haynes 160	146	15	131	3
Sanicro 28	-*	-*	-*	-*
Haynes 556	157	67	90	2
IN 625	771	742	29	1

*Sanicro 28 gave a wide variation in results and shape of plots.

Table 16. Pitting Potential, Repassivation Potential and Hysteresis in Reverse Polarisation Results for Materials in NaCl/$FeCl_2$ at 30ºC.

Alloy	E_{np} (mV(SCE))	E_{cp}(mV(SCE))	E_{cp}- E_{cp} (mV)	Rank
AISI 316L	*	*	361	6
Alloy 800H	*	*	298	5
Haynes 556	*	*	130	4
Haynes 160	*	*	128	3
AISI 310	*	*	127	2
Sanicro 28	-	-	-	-
IN 625	934	818	116	1

* no clear pitting potential seen so hysteresis value taken at 0.01mA/cm^2.
Sanicro 28 gave a wide variation in results and shape of plots.

Table 17. Analysis of Char

Char	Weight %		
	Sample 1	Sample 2	Mean
C	56.8	56.7	56.48
H	0.7	0.7	0.70
N	0.46	0.46	0.46
S	0.38	0.34	0.36
Cl	0.66	0.65	0.65
Ash	41.4	41.7	41.35

Table 18. Analysis of Char Ash

Ash	Weight %		
	Sample 1	Sample 2	Mean
Si	17.6	17.9	17.8
Al	13.1	13.4	13.3
Fe	5.0	5.1	5.1
Ca	13.9	14.1	14.0
Mg	1.1	1.1	1.1
Na	1.0	1.0	1.0
K	1.8	1.6	1.7
Ti	0.6	0.6	0.6

Table 19. Deposit Compositions Used

Deposit	Weight %									Chloride (moles)*
	Char	Ash	NaCl	KCl	$FeCl_2$	$FeCl_3$	PbS	ZnS	Cl	
1 (L)	90.00	-	3.74	-	6.26	-	-	-	6.36	1.06
2 (L)	90.00	-	2.00	1.0	2.00	-	4.0	1.0	3.39	0.38
3 (H)	-	90.00	3.74	-	6.26	-	-	-	5.77	0.96
4 (L)	90.00	-	3.74	-	-	6.26	-	-	6.96	1.40

L = Low H_2S gas, H = High H_2S gas
(* calculated using moisture content given in Table 21.)

Table 20. Measured Moisture Contents of Simulated Deposits.

Deposit	Mean weight of water per unit dry deposit (g/g)
1 (30°C)	0.65
2 (30°C)	0.46
3 (30°C)	0.65
4 (30°C)	0.70

Table 21. DTC Test Results in Terms of Degradation Type for Deposit 1 (in parenthesis depth of attack (μm))

Alloy	Downtime Corrosion Exposure Time (hours)						PRENW	Rank
	25	50	75	100	145 [1]	175 [2]		
Alloy 800H	CI	CI (235)	CI (>400)	CI (>400)	-	CI (>400)	21.0	6
AISI 316L	C - bands of attack	C (30)	CP (138)	CP (255)	-	CI (278)	24.0	5
AISI 310	P	P (13)	P (13) - pit no. increasing	-	P (14)	-	25.0	4
Haynes 160	P -few isolated	P (46)	P (45)	-	P (46)	-	29.7	3
Sanicro 28	N/C	P (10) - edges	P (14)	-	P (15)	-	38.6	2
Haynes 556	N/C	N/C	N/C	-	N/C	-	38.0	1
IN 625	N/C	N/C	N/C	-	N/C	-	51.2	

(N/C = no change, P = pitting, C = crevice and I = intergranular attack), [1] after 70 hour cycle, [2] after 75 hour cycle.

Table 22. DTC Test Results in Terms of Degradation Type for Deposit 2 (in parenthesis is depth of attack in μm)

Alloy	Downtime Corrosion Exposure Time (hours)				PRENW	Rank
	25	50	75	145 [1]		
Alloy 800H	CI (56)	CI (60)	CI (300)	N/C	21.0	5
AISI 316L	C (18), stained	C (22), stained	C (32), stained	N/C	24.0	4
Haynes 160	P (32), (2 pits) stained	N/C	N/C	N/C	29.7	3
Sanicro 28	Slightly stained	N/C	N/C	N/C	38.6	2
AISI 310	N/C	N/C	N/C	N/C	25.0	1
Haynes 556	N/C	N/C	N/C	N/C	38.0	
IN 625	N/C	N/C	N/C	N/C	51.2	

(N/C = no change, P = pitting, C = crevice and I = intergranular attack), [1] after 70 hour cycle

Table 23. Classification of Corrosion Inhibitors [48]

Type	Example Species	Further Classification
Anodic [1]	Chromate, Nitrite	Oxidising Passivator
	Phosphate, Molybdate, Tungstate	Non-Oxidising Passivator
Cathodic [2]	Arsenates	Cathodic Poison
	Carbonates, Zinc Sulphate	Precipitates
Precipitation	Phosphates, Silicates	Anodic/Cathodic Effects
Oxygen Scavenger	Sulphite, Hydrazine	Cathodic
Volatile/Vapour Phase	Cyclohexamines	Passivating
	Morpholine	Neutralising
Film-Forming [3]	Amines, Imidazolines, Quaternaries, Acetylenic Alcohols	Organic/Adsorption

[1] Sometimes refereed to as 'dangerous' inhibitors because of a need to be present above critical concentrations if the promotion of pitting corrosion is to be avoided.
[2] Sometimes refereed to as 'safe' inhibitors because they do not directly interfere with the anodic reaction but reduce the net current flowing in the overall corrosion reaction.
[3] May well exhibit anodic, cathodic or mixed behaviour.

Table 24. Damage Observed/Measured on DTC Specimens Exposed to DTC Test with and Without 1% Thiourea Inhibitor for 50 to 100 Hours (* PRENW value).

Alloy	With inhibitor (100 hours)	Without inhibitor (50 hours)
T23 *(n/a)	Shedding layers of rust.	Shedding layers of rust
347H *(17-20)	Surface covered by fine pitting and has 'dry river bed appearance', maximum 4µm deep	5 large very round pits, typically 175µm wide and 138µm deep. Area near edge where a number of pits have joined together, 700 x 575µm wide and 190µm deep.
Esshete 1250 *(17-20)	Surface has 'over-etched appearance', maximum 3µm deep.	7 large round pits, maximum 275µm wide and 118µm deep.
800HT *(19-23)	Fine pitting around edges, maximum 14µm wide and 2µm deep.	Fine pitting around edges with areas where pits have joined together, maximum 255 x 130µm wide and 54µm deep
AISI 316L *(23-28)	Surface covered by fine pits with some joining together, maximum 10µm wide and 6µm deep.	Surface covered by fine pits with some joining together, particularly in one central area to give region 165 x 250µm wide and 90µm deep
AISI 310 *(24-26)	Well distributed fine pitting that have joined in areas, typically 20µm wide and 8µm wide, maximum 130µm wide and 56µm deep.	Surface covered in small pits with regions where pits have possibly joined maximum 175 x 145µm wide and 40µm deep.
HR160 *(30)	A few isolated pits, typically 26µm wide and 3µm deep	A few isolated pits, typically 20µm wide and 2µm deep
Sanicro 28 *(36-41)	Fine pitting over surface, typically 16µm wide and 1µm deep.	Fine pitting over surface, typically 16µm wide and 1µm deep.
Haynes 556 *(39)	One pit 40µm wide and 6µm deep	No damage observed.
Inconel 625 *(51)	No damage observed.	No damage observed.

Table 25. H_2S Gas Composition

Gas	Gas Compositions (vol.%)							
	CO	CO_2	H_2	H_2S	H_2O	HCl	CH_4	N_2
'High H_2S'	61.0	4.00	31.0	1.00	3.00	0.04	-	-
'Low H_2S'	18.0	8.4	14.7	0.02	10.4	0.06	2.5	Bal

Table 26. Test Matrix

No	Test	T (ºC)	Gas	Deposit	HTGC	DTC
1	1a	450	High	High	○	○
2					○	
3	1b			None	○	○
4					○	
5	3a		Low	Low	○	○
6					○	
7	3b			None	○	○
8					○	
9	2a	550	High	High	○	○
10					○	
11	2b			None	○	○
12					○	
13	4a		Low	Low	○	○
14					○	
15	4b			None	○	○
16					○	

Table 27. Summary of Results of Applying a Failure Criteria of 20µm to Typical Oxide Measurements

Number	**1**	**2**	**3**	**4**	**5**	**6**	**7**	**8**	**9**	**10**	**11**	**12**	**13**	**14**	**15**	**16**
Temperature	**450ºC**								**550ºC**							
Gas	**High H_2S**				**Low H_2S**				**High H_2S**				**Low H_2S**			
Deposit	✓		✖		✓		✖		✓		✖		✓		✖	
DTC	✓	✖	✓	✖	✓	✖	✓	✖	✓	✖	✓	✖	✓	✖	✓	✖
AISI 316L	✓	✓	✖	✓	✓	✓	✓	✓	✖	✖	✖	✖	✓	✓	✓	✓
AISI 310	✖	✓	✓	✓	✓	✓	✓	✓	✖	✓	✓	✓	✓	✓	✓	✓
AISI 347	✓	✖	✖	✓	✓	✓	✓	✓	✖	✖	✖	✖	✓	✓	✓	✓
Alloy 800	✖	✖	✓	✓	✓	✓	✓	✓	✖	✖	✖	✖	✓	✓	✓	✓
Sanicro 28	✓	✓	✓	✓	✓	✓	✓	✓	✖	✖	✓	✓	✓	✓	✓	✓
HR160	✓	✓	✓	✓	✓	✓	✓	✓	✓	✖	✓	✖	✓	✓	✓	✓
Esshete 1250	✖	✖	✖	✓	✓	✓	✓	✓	✖	✖	✖	✖	✓	✓	✓	✓
Haynes 556	✓	✓	✓	✓	✓	✓	✓	✓	✖	✓	✖	✓	✓	✓	✓	✓
IN 625	✓	✓	✓	✓	✓	✓	✓	✓	✖	✖	✖	✖	✓	✓	✓	✓
T23	✖	✖	✖	✖	✖	✖	✖	✖	✖	✖	✖	✖	✖	✖	✖	✖

Table 28. Summary of Results of Applying a Failure Criteria of 20µm to Maximum Oxide Measurements

Number	**1**	**2**	**3**	**4**	**5**	**6**	**7**	**8**	**9**	**10**	**11**	**12**	**13**	**14**	**15**	**16**
Temperature	**450ºC**								**550ºC**							
Gas	**High H_2S**				**Low H_2S**				**High H_2S**				**Low H_2S**			
Deposit	✓		✖		✓		✖		✓		✖		✓		✖	
DTC	✓	✖	✓	✖	✓	✖	✓	✖	✓	✖	✓	✖	✓	✖	✓	✖
AISI 316L	✖	✖	✖	✖	✓	✓	✓	✓	✖	✖	✖	✖	✓	✓	✓	✓
AISI 310	✖	✖	✖	✖	✓	✓	✓	✓	✖	✖	✖	✖	✓	✓	✓	✓
AISI 347	✖	✖	✖	✖	✓	✓	✓	✓	✖	✖	✖	✖	✓	✓	✓	✓
Alloy 800	✖	✖	✖	✖	✓	✓	✖	✓	✖	✖	✖	✖	✓	✓	✖	✓
Sanicro 28	✓	✓	✓	✓	✓	✓	✓	✓	✖	✖	✖	✖	✓	✓	✓	✓
HR160	✓	✓	✓	✓	✓	✓	✓	✓	✖	✖	✓	✖	✓	✓	✓	✓
Esshete 1250	✖	✖	✖	✖	✓	✓	✓	✓	✖	✖	✖	✖	✓	✖	✓	✓
Haynes 556	✓	✓	✖	✓	✓	✓	✓	✓	✖	✓	✖	✓	✓	✓	✓	✓
IN 625	✖	✖	✖	✓	✓	✓	✓	✓	✖	✖	✖	✖	✓	✓	✓	✓
T23	✖	✖	✖	✖	✖	✖	✖	✖	✖	✖	✖	✖	✖	✖	✖	✖

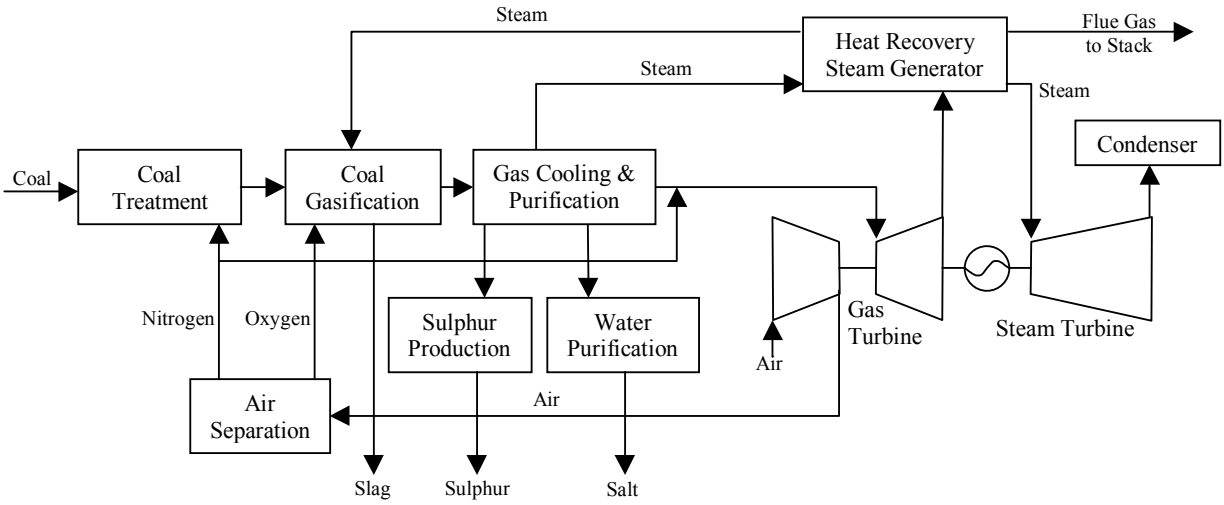

Figure 1. Entrained Flow Coal Gasification Process

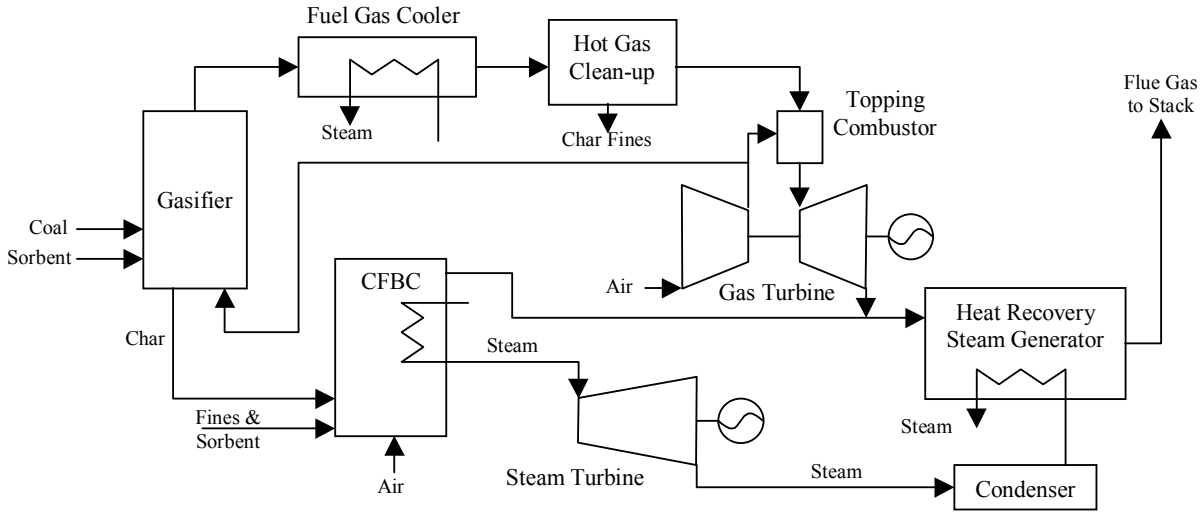

Figure 2. Air Blown Gasification Cycle

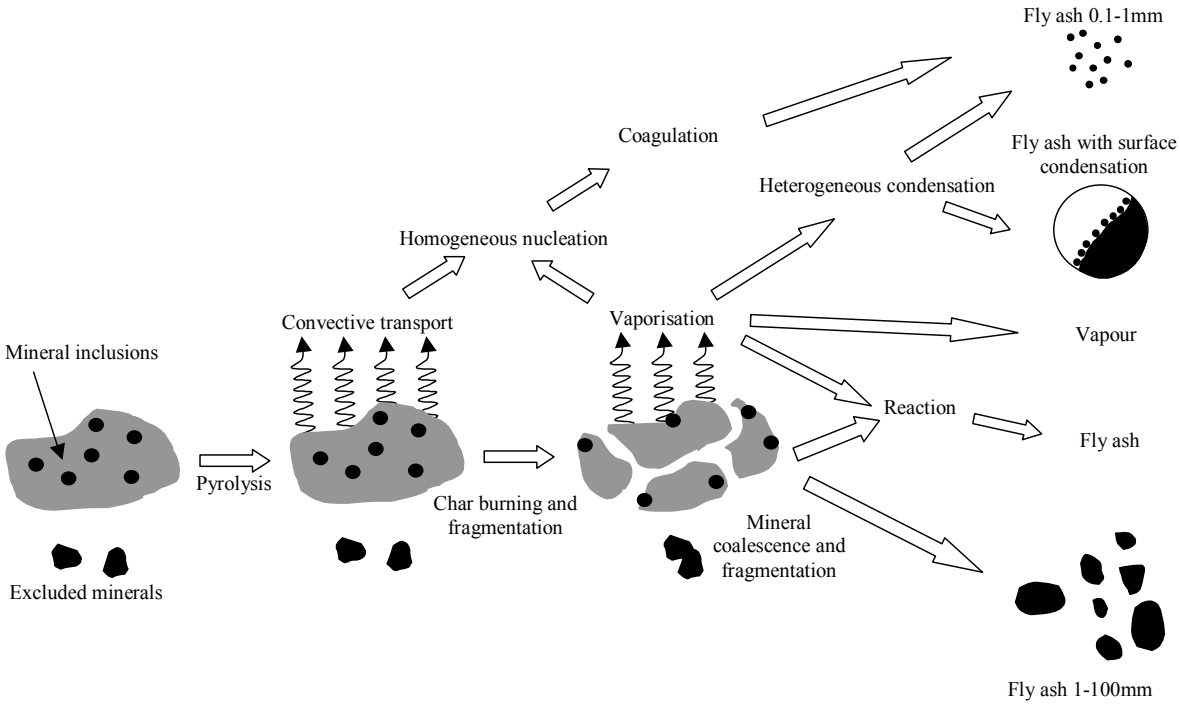

Figure 3. Schematic Diagram of the Breakdown of a Piece of Coal during Gasification

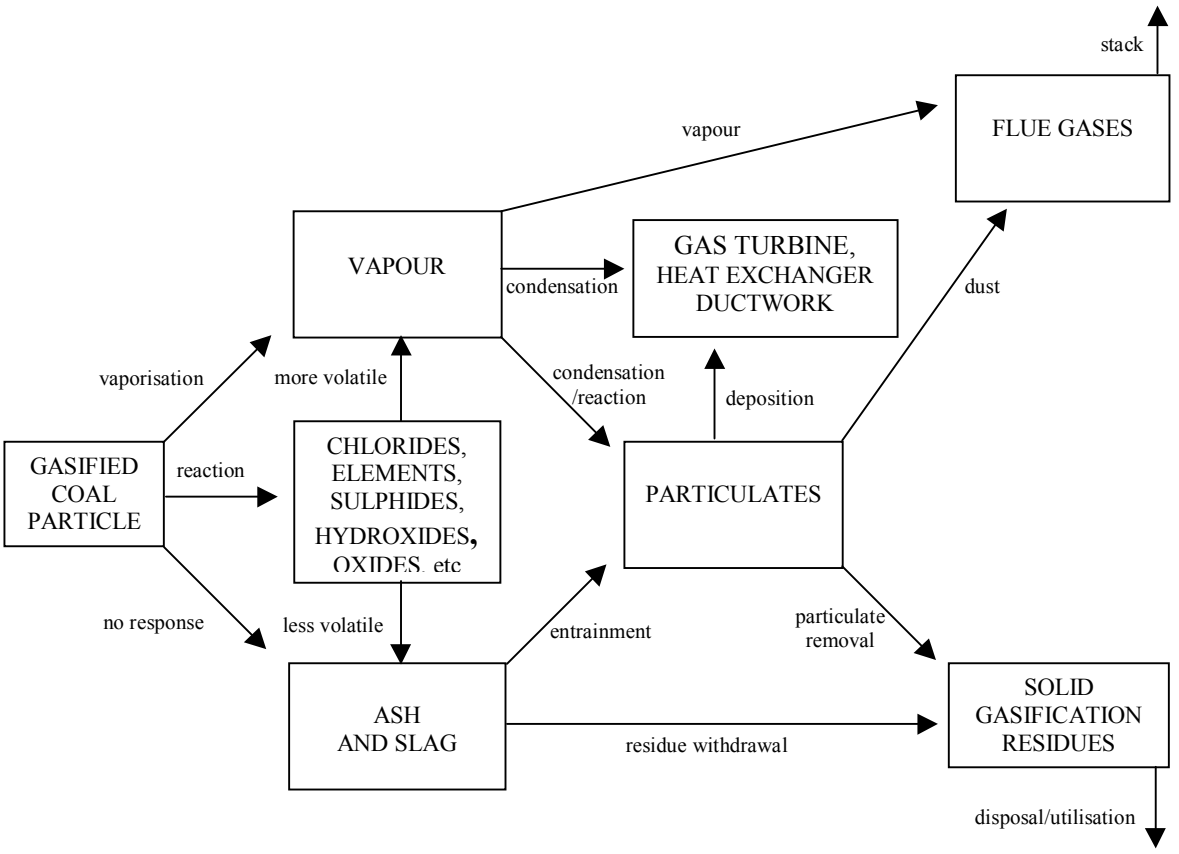

Figure 4. Fate of elements in a coal gasification system

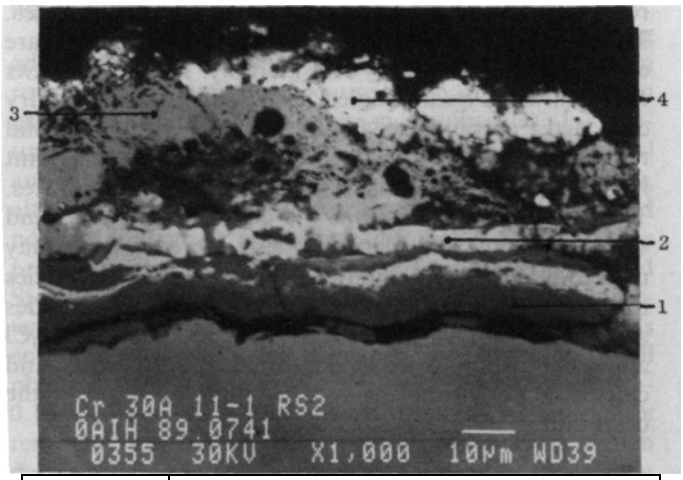

Element	Concentration			
	Area 1	Area 2	Area 3	Area 4
Se				4.3
Si				1.5
S	10.8	1.6	0.2	12.9
Ti	0.4			
Cr	69.0	4.4	0.9	0.3
Fe	6.1	2.7	7.7	0.7
Ni	2.9	31.4	30.3	
Ge	2.0	2.6	8.3	
As	0.9	8.1	43.2	
Mo	5.0			
Pb	3.0			80.4
Sb		49.7	9.4	

Figure 5. Condensed Trace Element Deposits on Heat Exchanger Tube From an Entrained Slagging Coal Gasifier with a Metal Temperature of ~425°C.

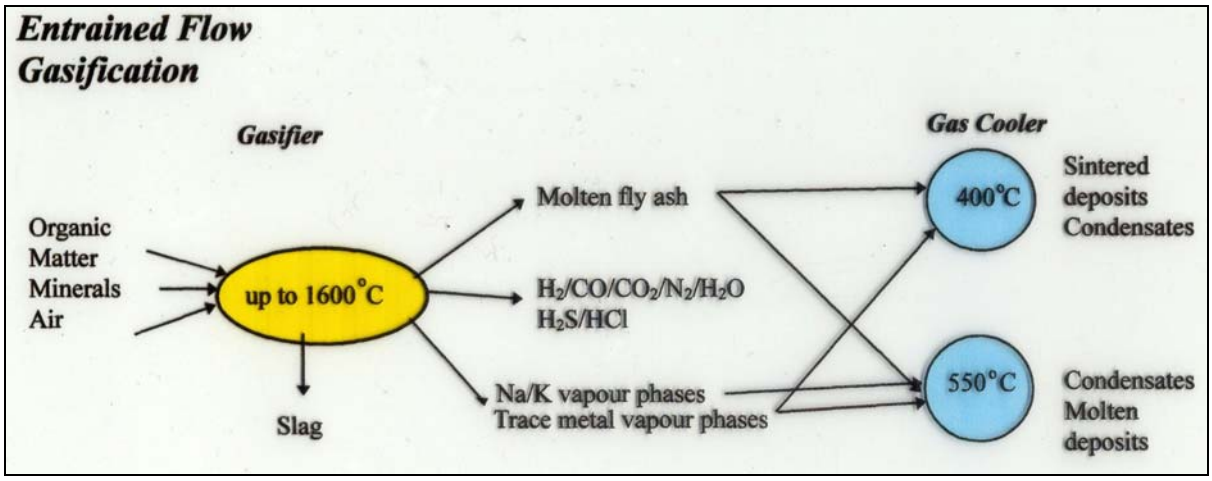

Figure 6. Formation of Deposition on Evaporator and Superheater Heat Exchanger Surfaces in Entrained Gasification Systems

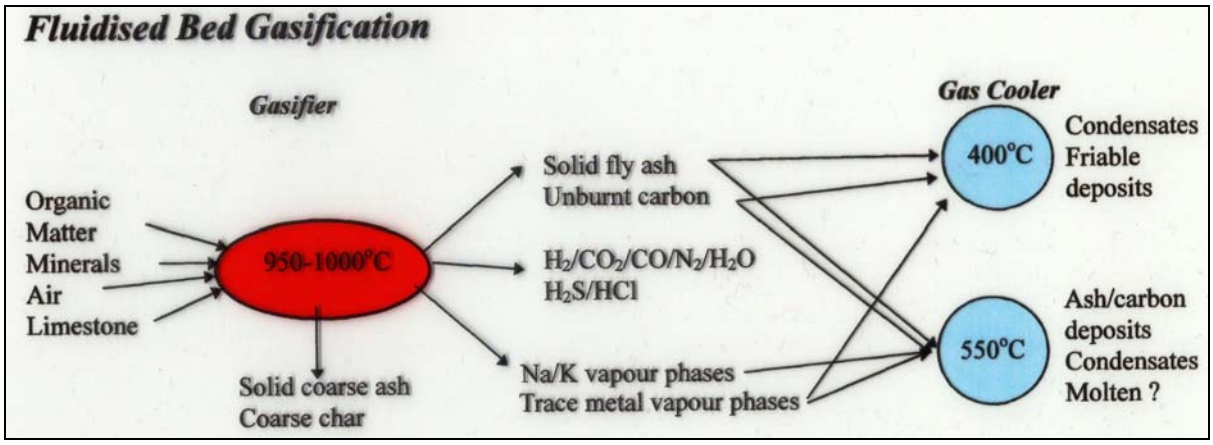

Figure 7. Formation of Deposition on Evaporator and Superheater Heat Exchanger Surfaces in Entrained Gasification Systems

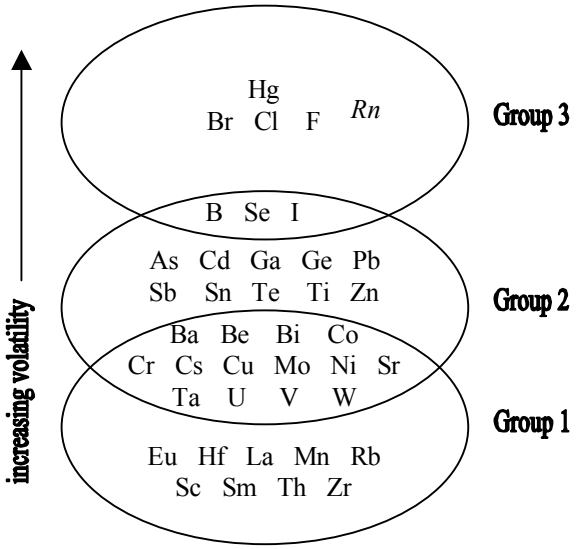

Figure 8. Classification of Trace Elements by Their Behaviour During Combustion and Gasification (after Clarke [16, 36]). Group 1: Equally Distributed Between Bottom Ash and Fly Ash, Group 2: Enriched in the Fly Ash and Depleted in the Bottom Ash, Group 3: Volatised and Emitted Fully in the Vapour Phase, Not Enriched in the Fly Ash.

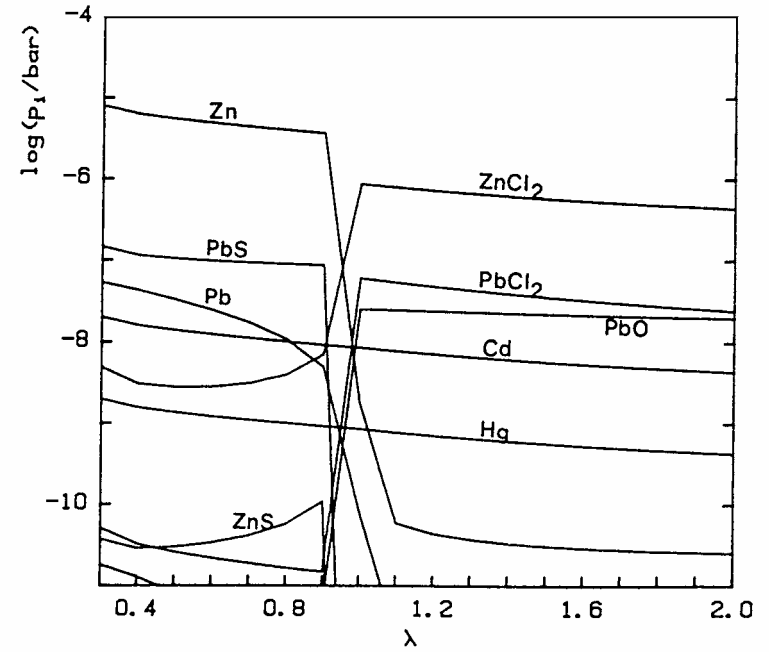

Figure 9. Variation of the partial pressure of some gaseous zinc, lead, cadmium and mercury species with λ for low sulphur coal at 850°C and 1bar [26].

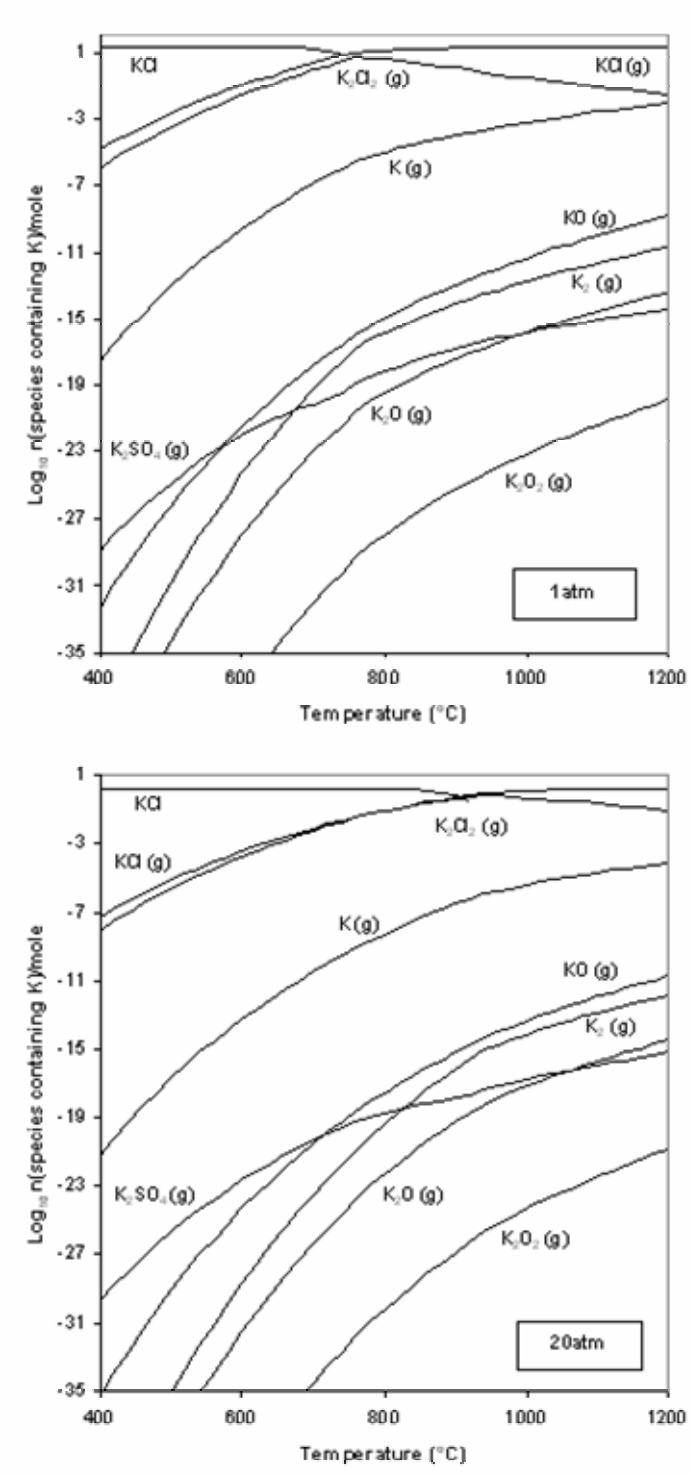

Figure 10. Effect of Pressure on Equilibrium Diagram for Potassium in ABGC gas.

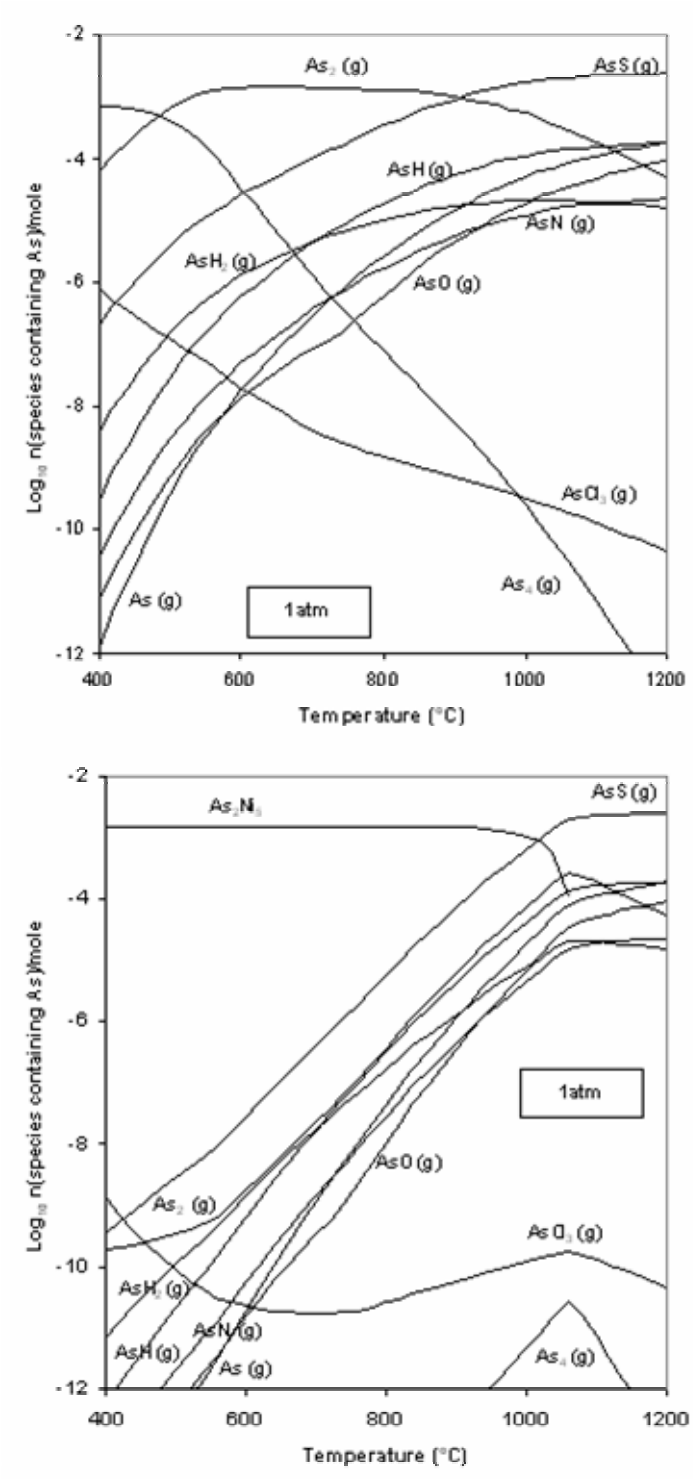

Figure 11. Effect of Nickel on Equilibrium Diagram for Arsenic in ABGC gas.

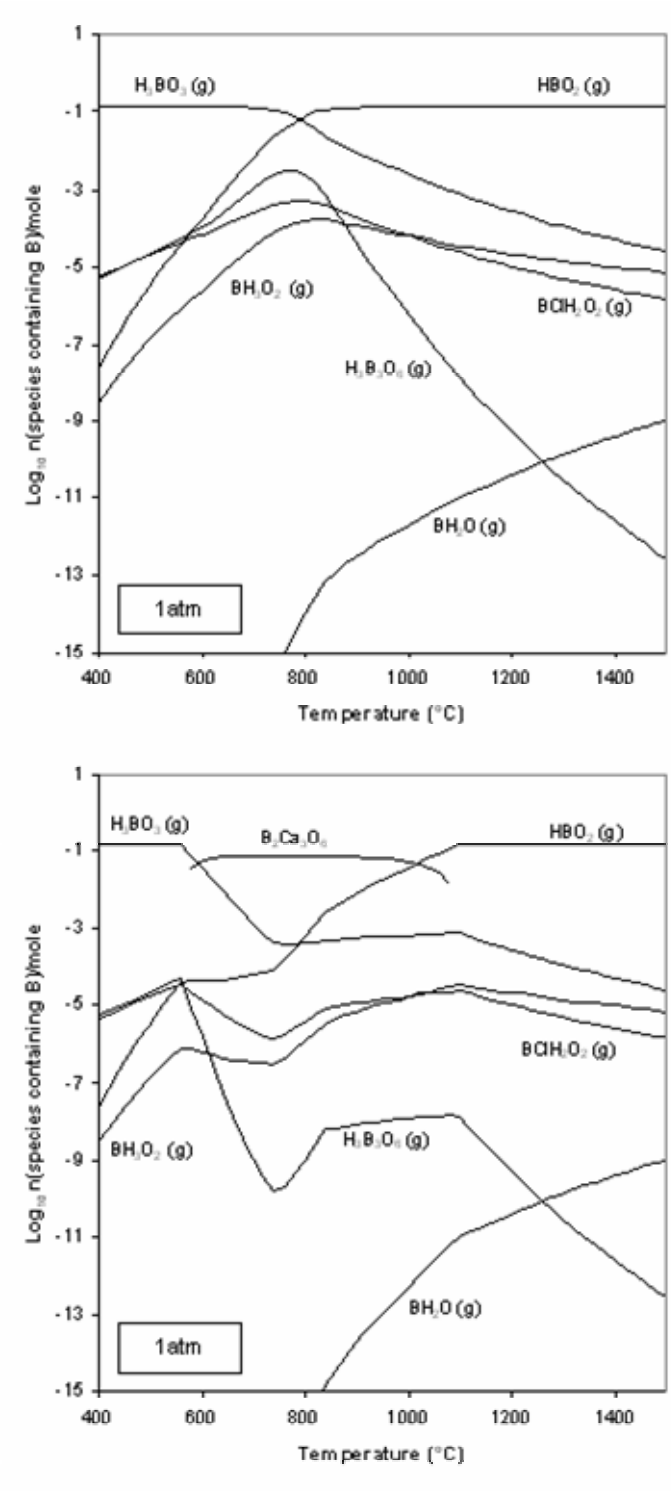

Figure 12. Effect of Calcium on Equilibrium Diagram for Boron in Prenflo Gas